

UNCLASSIFIED

AD NUMBER

AD887565

LIMITATION CHANGES

TO:

Approved for public release; distribution is unlimited.

FROM:

Distribution authorized to U.S. Gov't. agencies only; Test and Evaluation; SEP 1971. Other requests shall be referred to Armament Development and Test Center, Eglin AFB, FL.

AUTHORITY

AFATL ltr 24 Jun 1974

THIS PAGE IS UNCLASSIFIED

AEDC-TR-71-179  
AFATL-TR-71-114

cy 2



# SEPARATION CHARACTERISTICS OF THE PAVE STORM I AND II FROM THE F-4C AIRCRAFT AT MACH NUMBERS FROM 0.50 TO 0.95

A. C. Mansfield

ARO, Inc.

September 1971

This document has been approved for public release  
its distribution is unlimited.

*Per TAB 74-17,  
A2 16 August 74*

Distribution limited to U. S. Government agencies only;  
this report contains information on test and evaluation  
of military hardware; September 1971; other requests  
for this document must be referred to Armament  
Development and Test Center (DLGC), Eglin AFB,  
Florida 32542.

**PROPULSION WIND TUNNEL FACILITY  
ARNOLD ENGINEERING DEVELOPMENT CENTER  
AIR FORCE SYSTEMS COMMAND  
ARNOLD AIR FORCE STATION, TENNESSEE**

PROPERTY OF U S AIR FORCE  
AEDC LIBRARY  
F40600-72-C-0003

# ***NOTICES***

When U. S. Government drawings specifications, or other data are used for any purpose other than a definitely related Government procurement operation, the Government thereby incurs no responsibility nor any obligation whatsoever, and the fact that the Government may have formulated, furnished, or in any way supplied the said drawings, specifications, or other data, is not to be regarded by implication or otherwise, or in any manner licensing the holder or any other person or corporation, or conveying any rights or permission to manufacture, use, or sell any patented invention that may in any way be related thereto.

Qualified users may obtain copies of this report from the Defense Documentation Center.

References to named commercial products in this report are not to be considered in any sense as an endorsement of the product by the United States Air Force or the Government.

**SEPARATION CHARACTERISTICS OF THE  
PAVE STORM I AND II FROM THE F-4C AIRCRAFT  
AT MACH NUMBERS FROM 0.50 TO 0.95**

**A. C. Mansfield  
ARO, Inc.**

This document has been approved for public release  
its distribution is unlimited. *Per TAB 74-17,  
HIC 16 August, 74*

Distribution limited to U. S. Government agencies only;  
this report contains information on test and evaluation  
of military hardware; September 1971; other requests  
for this document must be referred to Armament  
Development and Test Center (DLGC), Eglin AFB,  
Florida 32542.

## FOREWORD

The work reported herein was sponsored by the Armament Development and Test Center, Air Force Armament Laboratory (DLGC), Air Force Systems Command (AFSC), under Program Element 64212F, Project 6033, Task 02.

The test results presented were obtained by ARO, Inc. (a subsidiary of Sverdrup & Parcel and Associates, Inc.), contract operator of the Arnold Engineering Development Center (AEDC), AFSC, Arnold Air Force Station, Tennessee, under Contract F40600-72-C-0003. The test was conducted from June 7 to 11, 1971, under ARO project No. PC0148. The manuscript was submitted for publication on July 20, 1971.

This technical report has been reviewed and is approved.

George F. Garey  
Lt Colonel, USAF  
AF Representative, PWT  
Directorate of Test

Joseph R. Henry  
Colonel, USAF  
Director of Test

## ABSTRACT

Wind-tunnel tests were conducted using 0.05-scale models to investigate the separation characteristics of the Pavestorm I and II munitions from the F-4C aircraft. The separation trajectories were initiated from the right-wing inboard pylon. Captive-trajectory store-separation data were obtained at Mach numbers from 0.50 to 0.95 for the parent aircraft in level flight, and 30- and 60-deg dive angles at a simulated altitude of 5000 ft. For the time period of the trajectories obtained, the store separated from the parent aircraft without store-to-parent contact.

This document has been approved for public release  
its distribution is unlimited.

*74-17  
Rey TAB  
DLG 16 August, 74*

Distribution limited to U. S. Government agencies only; this report contains information on test and evaluation of military hardware; September 1971; other requests for this document must be referred to Armament Development and Test Center (DLGC), Eglin AFB, Florida 32542.

## CONTENTS

	<u>Page</u>
ABSTRACT . . . . .	iii
NOMENCLATURE . . . . .	vi
I. INTRODUCTION . . . . .	1
II. APPARATUS	
2.1 Test Facility . . . . .	1
2.2 Test Articles . . . . .	2
2.3 Instrumentation . . . . .	2
III. TEST DESCRIPTION	
3.1 Test Conditions . . . . .	2
3.2 Trajectory Data Acquisition . . . . .	2
3.3 Corrections . . . . .	3
3.4 Precision of Data . . . . .	3
IV. RESULTS AND DISCUSSION . . . . .	4
REFERENCES . . . . .	5

## APPENDIXES

## I. ILLUSTRATIONS

Figure

1. Isometric Drawing of a Typical Store-Separation Installation and a Block Diagram of the Computer Control Loop . . . . .	9
2. Schematic of the Tunnel Test Section Showing Model Location . . . . .	10
3. Sketch of F-4C Parent-Aircraft Model . . . . .	11
4. Details and Dimensions of the F-4C Pylon Models . . . . .	12
5. Details and Dimensions of Pave Storm Models . . . . .	13
6. Details and Dimensions of the 370-gal Fuel Tank . . . . .	15
7. Tunnel Installation Photograph Showing Parent Aircraft with Store (Configuration 1) and CTS . . . . .	16
8. Aircraft/Weapons Loading Nomenclature . . . . .	17
9. Ejector Force Function for Inboard Pylon . . . . .	18
10. Mach Number Comparison of Pave Storm I Separation Trajectories for Different Dive Angles . . . . .	22
11. Mach Number Comparison of Pave Storm II Separation Trajectories for Different Dive Angles . . . . .	31
12. Dive Angle Comparison of Separation Trajectories . . . . .	40
13. Combined Mass and Center-of-Gravity Effects on Separation Trajectories for $M_\infty = 0.87$ and $\gamma = 0$ deg . . . . .	46
14. Effects of Reynolds Number Variation in the Wind Tunnel on the Trajectories for Configuration 4, $M_\infty = 0.70$ , $\alpha = 1.2$ , and $\gamma = 0$ . . . . .	48

## II. TABLES

I. Full-Scale Store Parameters Used in Trajectory Calculations . . . . .	49
II. Summary of Test Conditions . . . . .	50
III. Maximum Full-Scale Position Uncertainties Resulting from Balance Precision Limitations and Zero Shifts . . . . .	51

## NOMENCLATURE

BL	Aircraft buttock line form plane of symmetry, in., model scale
b	Store reference dimension, 1.688 ft, full scale
$C_{\ell}$	Store rolling-moment coefficient, rolling moment/ $q_{\infty}Sb$
$C_{\ell_p}$	Store roll-damping derivative, $dC_{\ell}/d(pb/2V_{\infty})$
$C_m$	Store pitching-moment coefficient, referenced to the store cg, pitching moment/ $q_{\infty}Sb$
$C_{m_q}$	Store pitch-damping derivative, $dC_m/d(qb/2V_{\infty})$
$C_n$	Store yawing-moment coefficient, referenced to the store cg, yawing moment/ $q_{\infty}Sb$
$C_{n_r}$	Store yaw-damping derivative, $dC_n/d(rb/2V_{\infty})$
c	Store reference length, 14.866 ft, full scale
FS	Aircraft fuselage station, in., model scale
$F_{Z_1}$	Pylon forward ejector force, lb, full scale
$F_{Z_2}$	Pylon aft ejector force, lb, full scale
H	Pressure altitude, ft
$I_{xx}$	Full-scale moment of inertia about the store $X_B$ axis, slug-ft sq
$I_{xz}$	Full-scale product of inertia, $X_B$ - $Z_B$ axis, slug-ft sq
$I_{yy}$	Full-scale moment of inertia about the store $Y_B$ axis, slug-ft sq
$I_{zz}$	Full-scale moment of inertia about the store $Z_B$ axis, slug-ft sq

$M_\infty$	Free-stream Mach number
$\bar{m}$	Full-scale store mass, slugs
$p$	Store angular velocity about the $X_B$ axis, radians/sec
$p_\infty$	Free-stream static pressure, psfa
$q$	Store angular velocity about the $Y_B$ axis, radians/sec
$q_\infty$	Free-stream dynamic pressure, psf
$Re$	Free-stream Reynolds number based on scale model diameter
$r$	Store angular velocity about the $Z_B$ axis, radians/sec
$S$	Store reference area, 2.237 sq ft, full scale
$t$	Real trajectory time from initiation of trajectory, sec
$V_\infty$	Free-stream velocity, ft/sec
$WL$	Aircraft waterline from reference horizontal plane, in., model scale
$X$	Separation distance of the store cg parallel to the flight-axis system $X_F$ direction, ft, full scale measured from the prelaunch position
$X_{cg}$	Full-scale cg location, ft, from nose of store
$X_{L_1}$	Forward ejector piston location relative to the store cg, positive forward of store cg, ft, full scale
$X_{L_2}$	Aft ejector piston location relative to the store cg, positive forward of store cg, ft, full scale
$Y$	Separation distance of the store cg parallel to the flight axis system $Y_F$ direction, ft, full scale measured from the prelaunch position
$Y_{cg}$	Full-scale cg location, ft, from the centerline in the body-axis system
$Z$	Separation distance of the store cg parallel to the flight-axis system $Z_F$ direction, ft, full scale measured from the prelaunch position
$Z_{cg}$	Full-scale cg location, ft, from centerline in the body-axis system
$\alpha$	Parent-aircraft model angle of attack relative to the free-stream velocity vector, deg

- $\gamma$  Simulated parent-aircraft dive angle. Angle between the flight direction and the earth horizontal, deg, positive for decreasing altitude
- $\theta$  Angle between the store longitudinal axis and its projection in the  $X_F$ - $Y_F$  plane, positive when store nose is raised as seen by pilot, deg
- $\psi$  Angle between the projection of the store longitudinal axis in the  $X_F$ - $Y_F$  plane and the  $X_F$  axis, positive when the store nose is to the right as seen by the pilot, deg
- $\phi$  Angle between the projection of the store lateral axis in the  $Y_F$ - $Z_F$  plane and the  $Y_F$  axis, positive for clockwise rotation when looking upstream, deg

## FLIGHT-AXIS SYSTEM COORDINATES

### Directions

- $X_F$  Parallel to the free-stream wind vector, positive direction is forward as seen by the pilot
- $Y_F$  Perpendicular to the  $X_F$  and  $Z_F$  directions, positive direction is to the right as seen by the pilot
- $Z_F$  In the aircraft plane of symmetry, perpendicular to the free-stream wind vector, positive direction is downward

The flight-axis system origin is coincident with the aircraft cg and remains fixed with respect to the parent aircraft during store separation. The  $X_F$ ,  $Y_F$ , and  $Z_F$  coordinate axes do not rotate with respect to the initial flight direction and attitude.

## STORE BODY-AXIS SYSTEM COORDINATES

### Directions

- $X_B$  Parallel to the store longitudinal axis, positive direction is upstream in the prelaunch position
- $Y_B$  Perpendicular to the store longitudinal axis, and parallel to the flight-axis system  $X_F$ - $Y_F$  plane when the store is at zero roll angle, positive direction is to the right looking upstream when the store is at zero yaw and roll angles
- $Z_B$  Perpendicular to both the  $X_B$  and  $Y_B$  axes, positive direction is downward as seen by the pilot when the store is at zero pitch and roll angles.

The store body-axis system origin is coincident with the store cg and moves with the store during separation from the parent airplane. The  $X_B$ ,  $Y_B$ , and  $Z_B$  coordinate axes rotate with the store in pitch, yaw, and roll so that mass moments of inertia about the three axes are not time-varying quantities.

## SECTION I INTRODUCTION

In the Aerodynamic Wind Tunnel (4T) of the Propulsion Wind Tunnel Facility (PWT), a captive-trajectory store-separation test was conducted to determine the characteristics of the Pavé Storm I and II munitions. The captive-trajectory test described herein dealt with the separation characteristic of 0.05-scale models of the Pavé Storm I and II as launched from the right-wing inboard pylon of the F-4C parent aircraft. The F-4C was mounted on the main tunnel support system, and the Pavé Storm stores were mounted on a strain-gage balance-and-sting combination attached to the captive-trajectory store-separation system (CTS). For Mach numbers from 0.5 to 0.95, flight conditions were simulated for an altitude of 5000 ft, parent-aircraft dive angles of 0, 30, and 60 deg, and variations in the full-scale mass configurations (Table I, Appendix II) of both Pavé Storm I and II.

## SECTION II APPARATUS

### 2.1 TEST FACILITY

The Aerodynamic Wind Tunnel (4T) is a closed-loop, continuous flow, variable density tunnel in which the Mach number can be varied from 0.2 to 1.3. At all Mach numbers, the stagnation pressure can be varied from 200 to 3400 psfa. The test section is 4 ft square and 12.5 ft long with perforated, variable porosity (0.5- to 10-percent open) walls. It is completely enclosed in a plenum chamber from which the air can be evacuated, allowing part of the tunnel airflow to be removed through the perforated walls of the test section.

For store-separation testing, two separate and independent support systems are used to support the models. The parent-aircraft model is inverted in the test section and supported by an offset sting attached to the main pitch sector. The store model is supported by the CTS which extends down from the tunnel top wall and provides store movement (six degrees of freedom) independent of the parent-aircraft model. An isometric drawing of a typical store-separation installation is shown in Fig. 1, Appendix I.

Also shown in Fig. 1 is a block diagram of the computer control loop used during captive-trajectory testing. The analog system and the digital computer work as an integrated unit and, utilizing required input information, control the store movement during a trajectory. Store positioning is accomplished by use of six individual d-c electric motors. Maximum translational travel of the CTS is  $\pm 15$  in. from the tunnel centerline in the lateral and vertical directions and 36 in. in the axial direction. Maximum angular displacements are  $\pm 45$  deg in pitch and yaw and  $\pm 360$  deg in roll. A more complete description of the test facility can be found in Ref. 1. A schematic showing the test section details and the location of the models in the tunnel is shown in Fig. 2.

## 2.2 TEST ARTICLES

The test articles were 0.05-scale models of the F-4C parent aircraft and Pavé Storm I and II stores. A sketch showing the basic dimensions of the F-4C parent model is shown in Fig. 3. For this test, the right-wing inboard pylon was equipped for store separation. The tail of the F-4C model was removed to provide clearance for the CTS. Details and dimensions of the pylon are shown in Fig. 4. The surfaces of the pylons are inclined nose down with respect to the aircraft waterline as indicated in Fig. 4.

Details and dimensions of the Pavé Storm I and II models are shown in Figs. 5a and b, respectively. The physical characteristics of the various configurations studied are given in Table I. A dimensional sketch of the 370-gal fuel tank used to obtain the desired aircraft configuration is shown in Fig. 6. The parent-aircraft model with stores and the CTS are shown in the installation photograph (Fig. 7).

## 2.3 INSTRUMENTATION

A six-component internal strain-gage balance was used to obtain store aerodynamic force and moment data. Translational and angular positions of the store were obtained from CTS analog outputs, while parent-model angle of attack was determined by an angular position indicator on the main pitch sector. The right-wing pylon contained a touch wire system which enabled the store to be accurately positioned for launch. The system was also wired to automatically stop the CTS motion and give visual indication should the store or sting support make contact with any surface other than the touch wire.

# SECTION III TEST DESCRIPTION

## 3.1 TEST CONDITIONS

Separation trajectory data were obtained at Mach numbers from 0.50 to 0.95. Table II presents the conditions for which the trajectories were obtained. The tunnel conditions were held constant at the desired Mach number and stagnation pressure while data for each trajectory were obtained.

Most trajectories were not run to the full limits of the CTS system. Generally, once the maximum initial pitch and yaw angle was obtained or once a complete half-cycle occurred, the trajectories were terminated. A few trajectories were run to the mechanical limits of the system.

## 3.2 TRAJECTORY DATA ACQUISITION

To obtain a trajectory, test conditions were established in the tunnel and the parent model was positioned at the desired angle of attack. The store model was then oriented to a position corresponding to the store-carriage location. After the store was set at the desired initial position, operational control of the CTS was switched to the digital computer.

which controlled the store movement during the trajectory through commands to the CTS analog system (see block diagram, Fig. 1). Data from the wind tunnel, consisting of measured model forces and moments, wind-tunnel operating conditions, and CTS rig positions were input to the digital computer for use in the full-scale trajectory calculations.

The digital computer was programmed to solve the six-degree-of-freedom equations to calculate the angular and linear displacements of the store relative to the parent-aircraft pylon (Ref. 2). In general, the program involves using the last two successive measured values of each static aerodynamic coefficient to predict the magnitude of the coefficients over the next time interval of the trajectory. These predicted values are used to calculate the new position and attitude of the store at the end of the time interval. The CTS is then commanded to move the store model to this new position and the aerodynamic loads are measured. If these new measurements agree with the predicted values, the process is continued over another time interval of the same magnitude. If the measured and predicted values do not agree within the desired precision, the calculation is redone over a time interval one-half the previous value. This process is repeated until a complete trajectory has been obtained.

In applying the wind-tunnel data to the calculations of the full-scale store trajectories, the measured forces and moments are reduced to coefficient form and then applied with proper full-scale store dimensions and flight dynamic pressure. Dynamic pressure was calculated using a flight velocity equal to the free-stream velocity component plus the components of store velocity relative to the aircraft, and a density corresponding to the simulated altitude.

The initial portion of each launch trajectory incorporated simulated ejector forces in addition to the measured aerodynamic forces acting on the store. The ejector force functions for the eight stores are presented in Fig. 9. The ejector force was considered to act perpendicular to the pylon mounting surface. The locations of the applied ejector forces and other full-scale store parameters used in the trajectory calculations are listed in Table II.

### 3.3 CORRECTIONS

Balance, sting, and support deflections caused by the aerodynamic loads on the store models were accounted for in the data reduction program to calculate the true store-model angles. Corrections were also made for model weight tares to calculate the net aerodynamic forces on the store model.

### 3.4 PRECISION OF DATA

The trajectory data are subject to error from several sources including tunnel conditions, balance measurements, extrapolation tolerances allowed in the predicted coefficients, computer inputs, and CTS position control, which was  $\pm 0.05$  in. for the translational settings and  $\pm 0.15$  for angular displacement settings in pitch and yaw. Extrapolation tolerances were  $\pm 0.10$  for each of the aerodynamic coefficients. The

uncertainties in full-scale position data caused by balance precision limitations and balance zero shifts are given in Table III. The uncertainty in setting Mach number was no greater than  $\pm 0.0095$  and the uncertainty in parent-model angle of attack was estimated to be  $\pm 0.1$  deg.

#### SECTION IV RESULTS AND DISCUSSION

Data obtained during this test consisted of ejector-initiated trajectories for the *Pave Storm I* and *II* munitions from the inboard pylon on the right wing of the F-4C aircraft. Data showing the linear displacements of the stores relative to the pylon position, and the angular displacements relative to the flight-axis system, are presented as functions of full-scale time in Figs. 10 through 13. Positive X, Y, and Z displacements (as seen by the pilot) are forward, to the right (outboard), and down, respectively. Positive changes in  $\psi$  and  $\theta$  (as seen by the pilot) are nose up and nose right (outboard), respectively. The termination of the trajectories was usually accomplished by monitoring pitch and yaw and stopping the trajectories after either the first peak or the first half-cycle. Some of the early trajectories on both the basic configurations (Configurations 1 and 4) were allowed to go to the Z limit of the CTS. Table II lists the full-scale store parameters used in the trajectory calculations and Fig. 8 describes the F-4C load configuration.

The ejector force functions used with the various store configurations were supplied by the sponsor (AFATL/ADTC) and are shown in Fig. 9.

Figures 10 and 11 present all the trajectory data for *Pave Storm I* and *II*, respectively, for the various Mach numbers and store weights. Generally, *Pave Storm I* (Fig. 10) separated with only small positive-pitch excursions and small negative-yaw excursions in the initial portions of the trajectories. *Pave Storm II* (Fig. 11) had large negative-pitch excursions and the yaw behavior was about the same as for *Pave Storm I*. There were some velocity effects on all variables. The primary one appeared to be the change in pitch and yaw frequencies for both *Pave Storm I* and *II*. There was also a change in roll direction with Mach number for *Pave Storm II*.

Figure 12 presents comparisons of the trajectory data for the basic Configurations 1 and 4, respectively, for dive angles of 0, 30, and 60 deg at constant Mach number. The main change in trajectories was seen to be in the X displacement, while the other parameters showed only minor deviations with dive angle.

The effects of changing the combined mass and center-of-gravity locations are presented in Fig. 13. As shown in Fig. 13a, the center-of-gravity movement was small and the dominant effect appears to have been the mass effect. In general, the frequencies of the angular rates and displacements showed expected effects of mass changes on the data. The center-of-gravity movement effect appeared to dominate the angular movements of the store as shown in Fig. 13b. The normal force produced by the pitch of the store combined with the mass changes would account for the different Z movements.

The effect of varying the test Reynolds number is shown in Fig. 14. The data indicate no significant effects on the trajectories from varying the Reynolds number. It is interesting to note that even at the low Reynolds number, the trajectories generally appear to repeat much better than would be expected for the indicated uncertainties in Table III.

#### REFERENCES

1. Test Facilities Handbook (Ninth Edition). "Propulsion Wind Tunnel Facility, Vol. 4." Arnold Engineering Development Center, July 1971.
2. Christopher, J. P. and Carleton, W. E. "Captive-Trajectory Store-Separation System of the AEDC-PWT 4-Foot Transonic Tunnel." AEDC-TR-68-200 (AD839743), September 1968.

**APPENDIXES**  
**I. ILLUSTRATIONS**  
**II. TABLES**

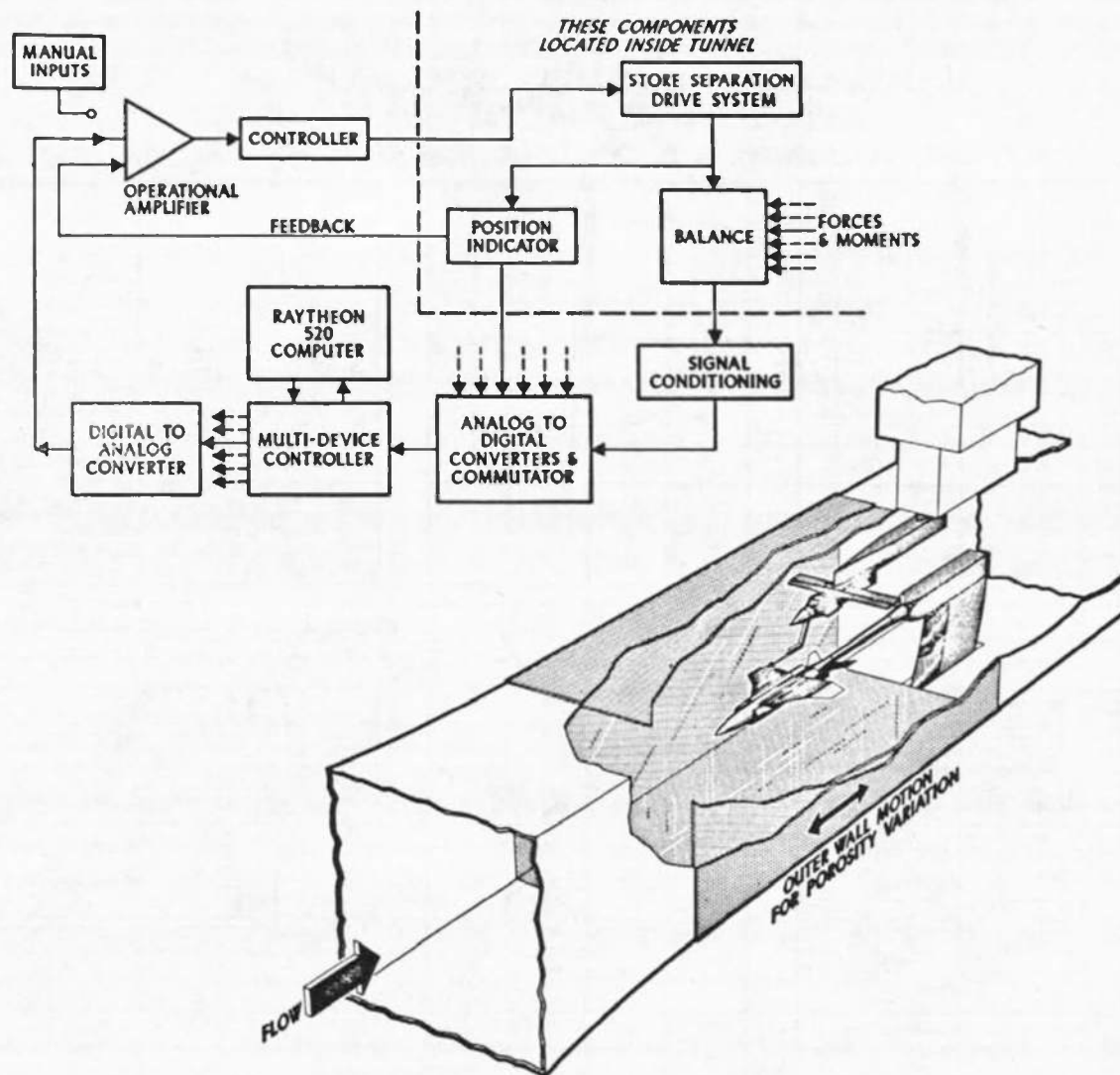
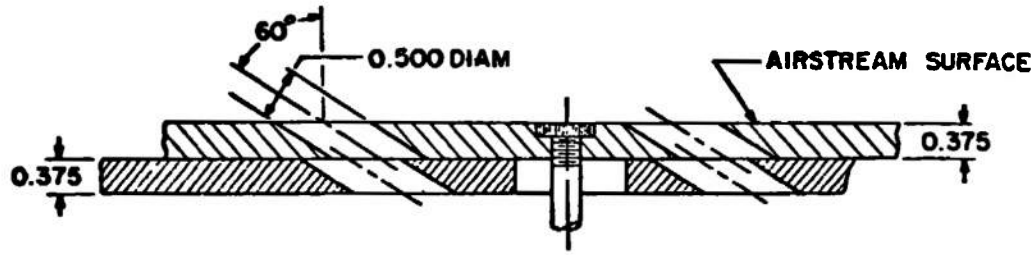


Fig. 1 Isometric Drawing of a Typical Store-Separation Installation and a Block Diagram of the Computer Control Loop



TYPICAL PERFORATED WALL CROSS SECTION

TUNNEL STATIONS AND DIMENSIONS ARE IN INCHES

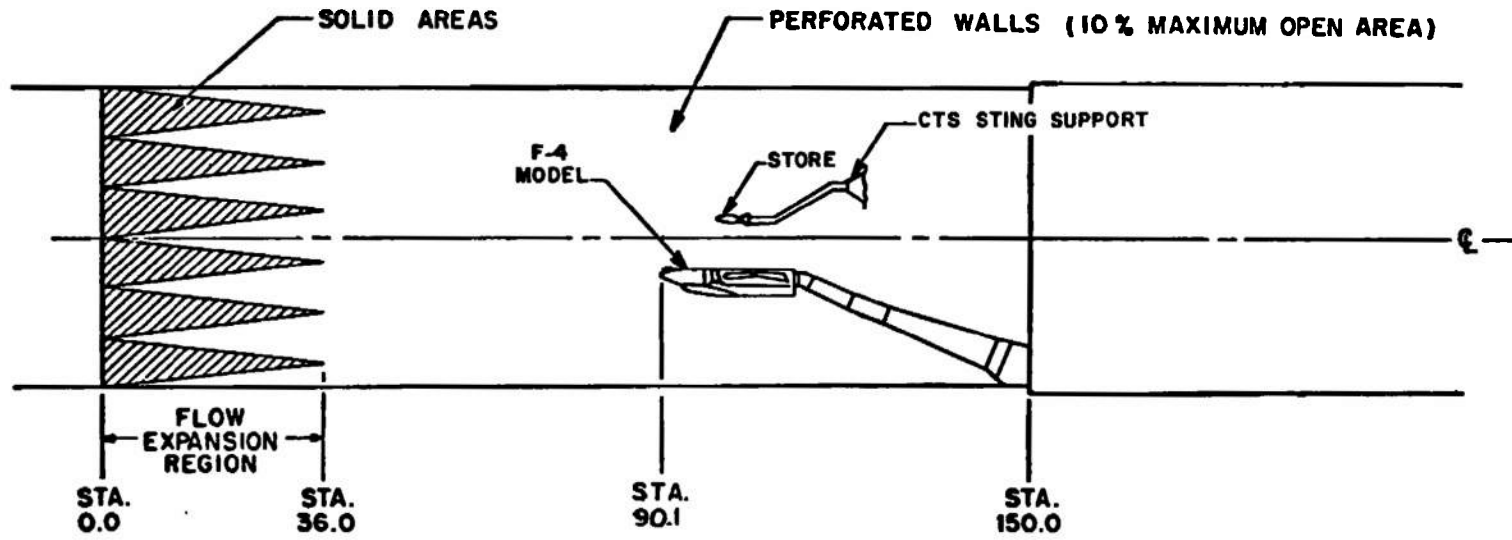


Fig. 2 Schematic of the Tunnel Test Section Showing Model Location

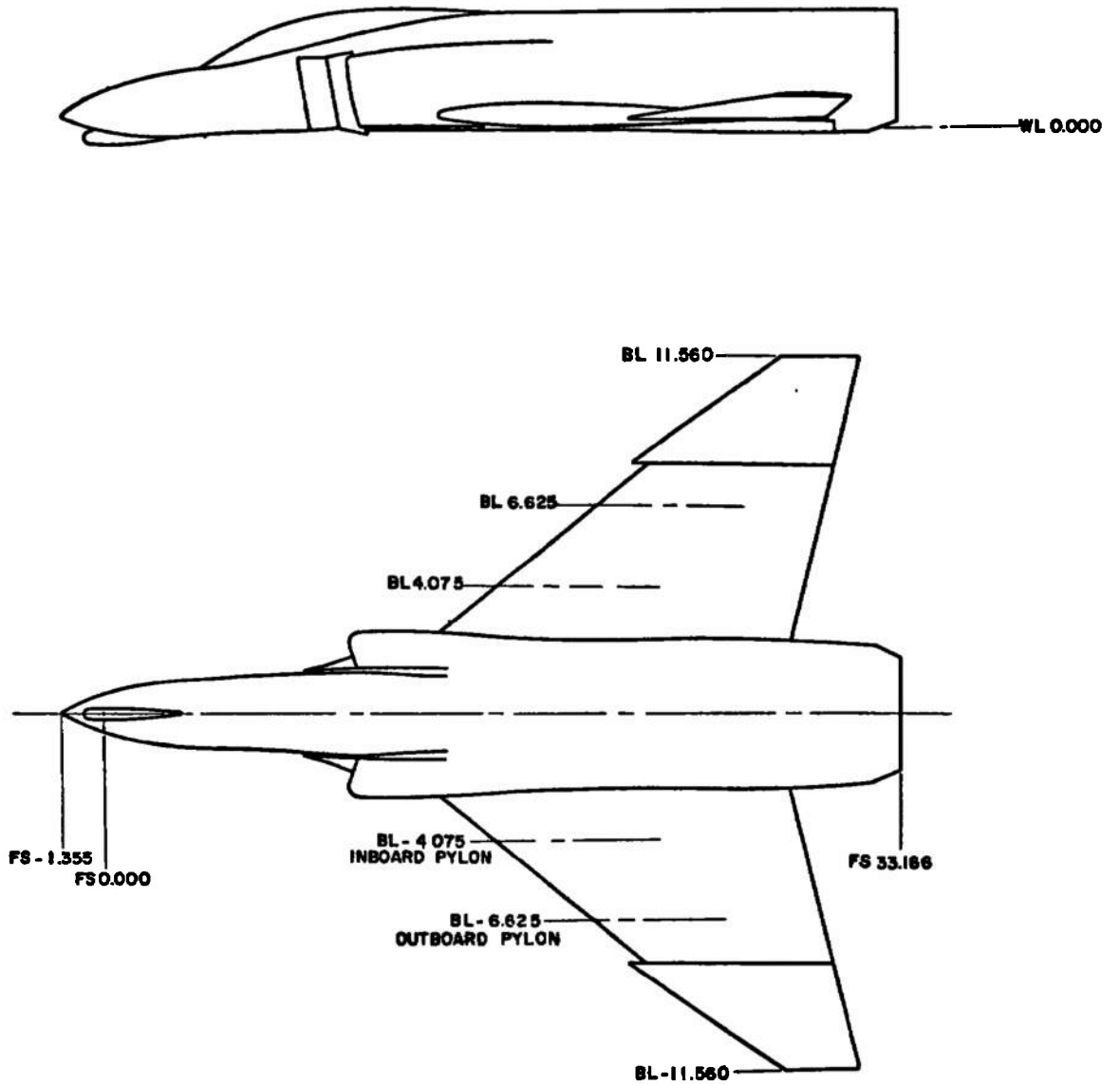
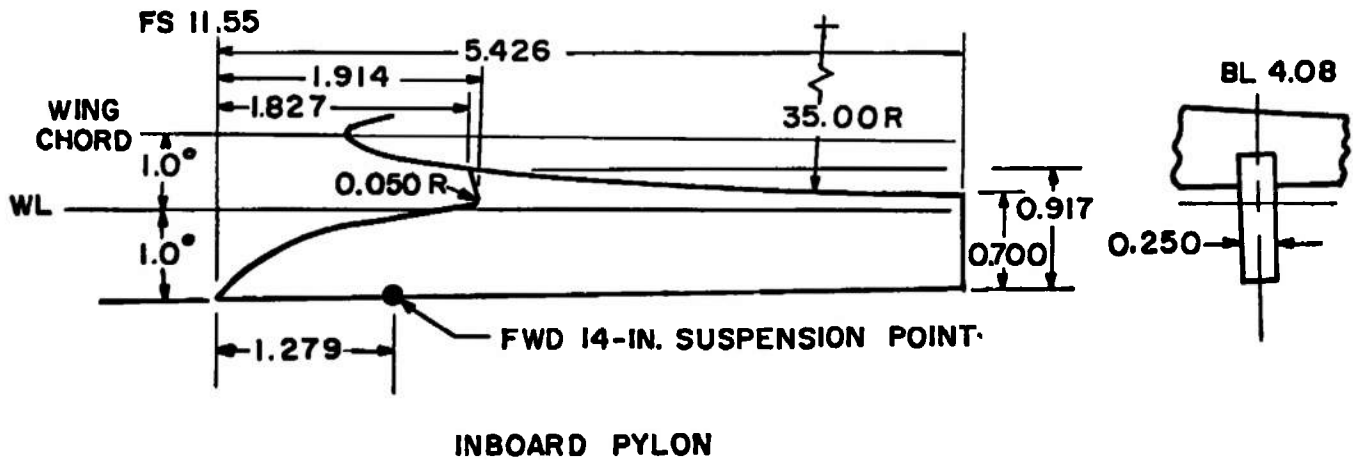
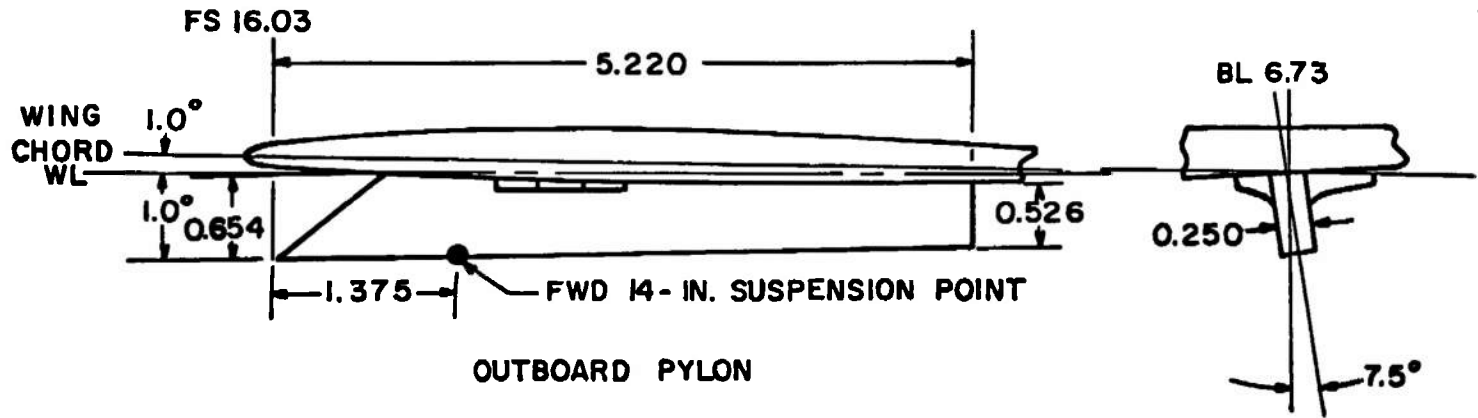
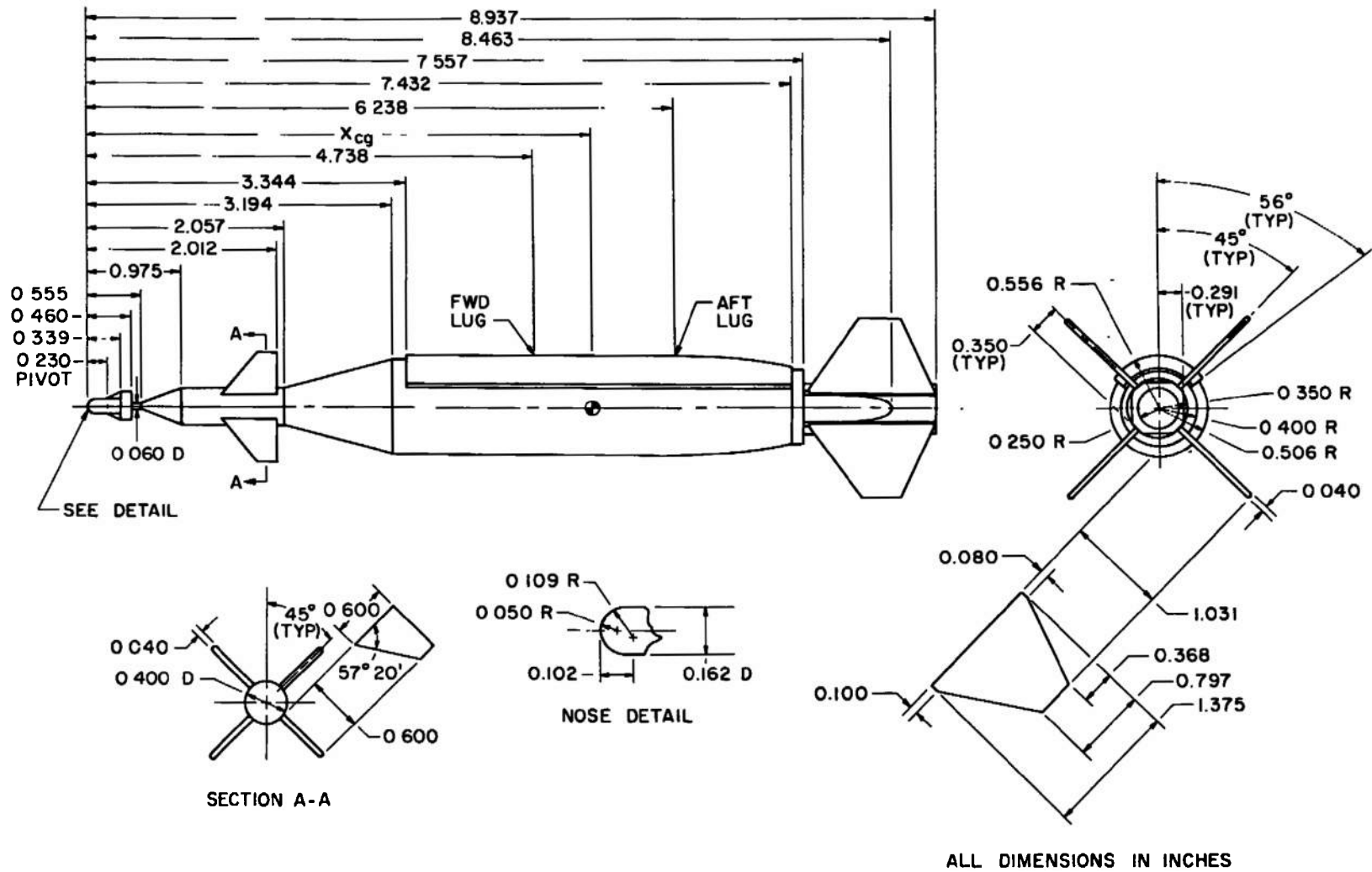


Fig. 3 Sketch of F-4C Parent-Aircraft Model

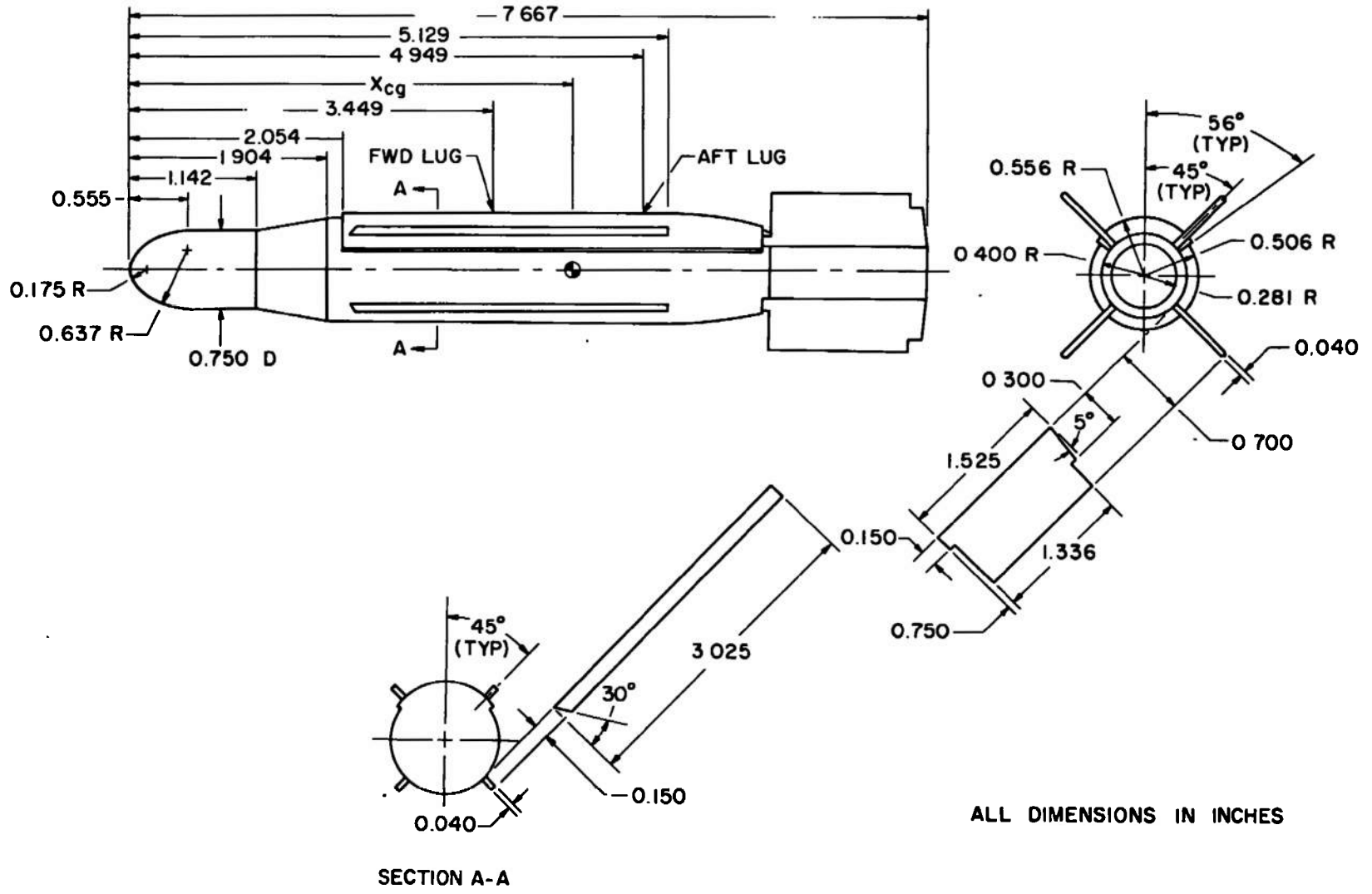


ALL DIMENSIONS IN INCHES

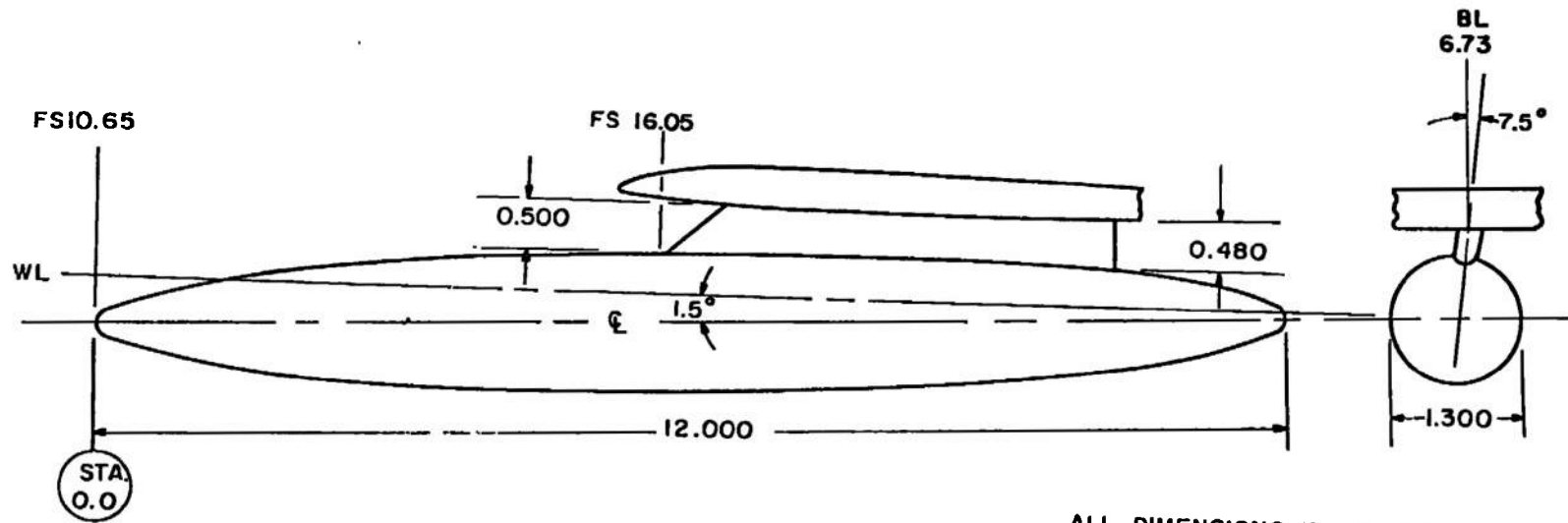
Fig. 4 Details and Dimensions of the F-4C Pylon Models



a. Pavé Storm I  
 Fig. 5 Details and Dimensions of Pavé Storm Models



b. Pave Storm II  
Fig. 5 Concluded



ALL DIMENSIONS IN INCHES

BODY CONTOUR, TYPICAL BOTH ENDS

STATION	BODY DIAM	STATION	BODY DIAM
0.000	0.000	2.500	1.116
0.025	0.100	2.750	1.156
0.050	0.144	3.000	1.190
0.150	0.258	3.250	1.218
0.250	0.340	3.500	1.242
0.500	0.498	3.750	1.260
0.750	0.622	4.000	1.274
1.000	0.724	4.250	1.286
1.250	0.812	4.500	1.294
1.500	0.890	4.750	1.298
1.750	0.958	5.000	1.300
2.000	1.016	6.000	1.300
2.250	1.070		

Fig. 6 Details and Dimensions of the 370-gal Fuel Tank

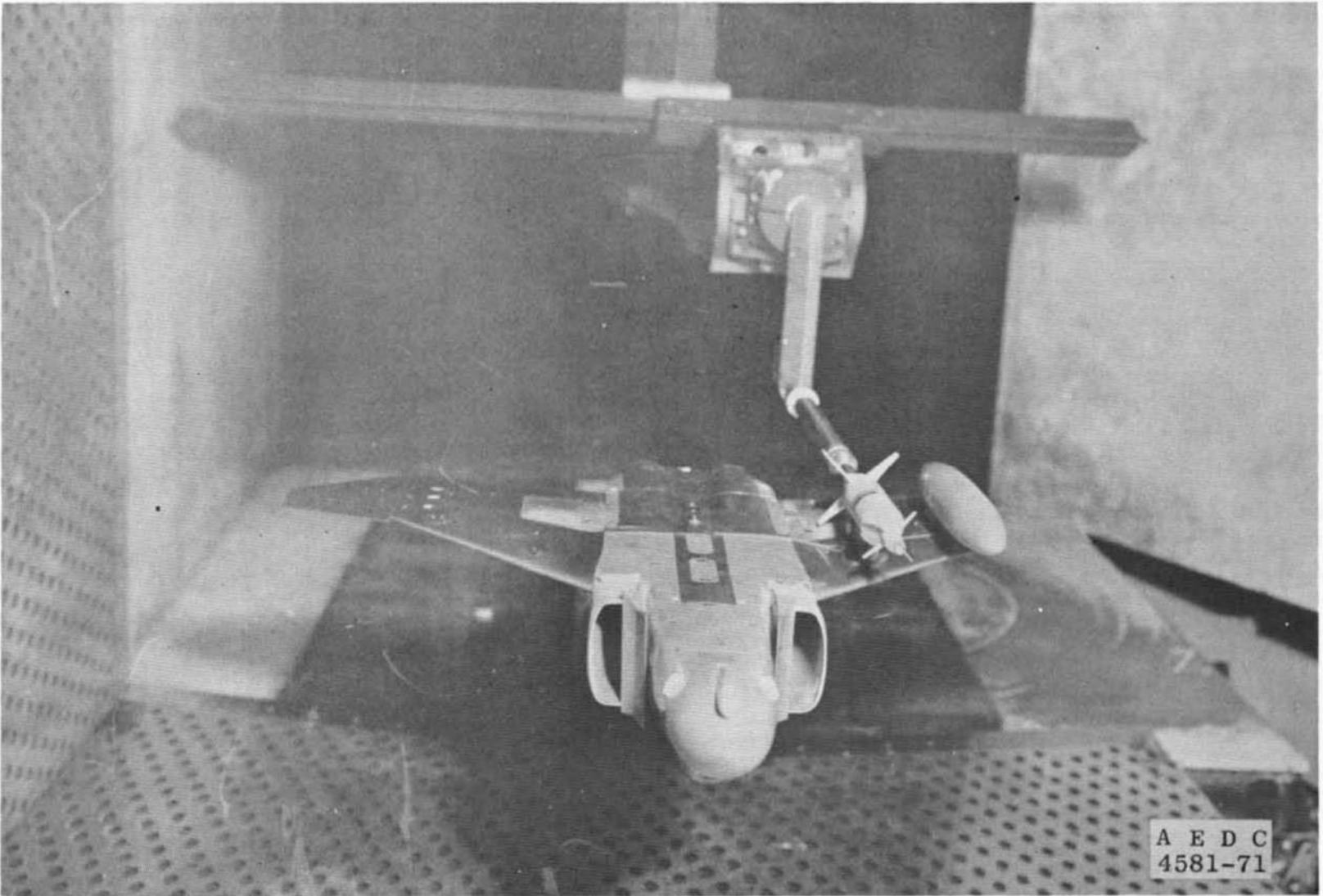


Fig. 7 Tunnel Installation Photograph Showing Parent Aircraft with Store (Configuration1) and CTS

LOOKING UPSTREAM

F - 4C

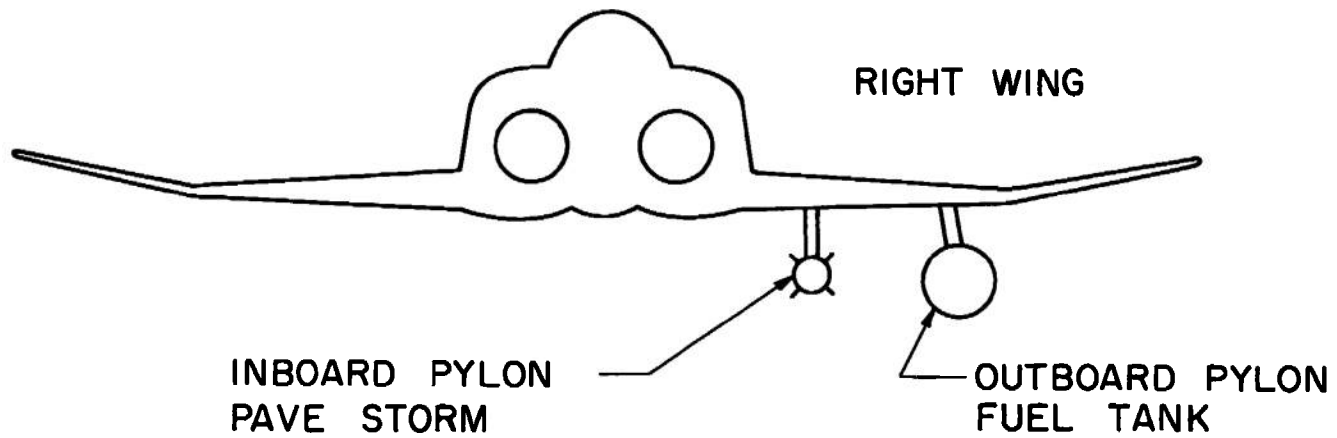
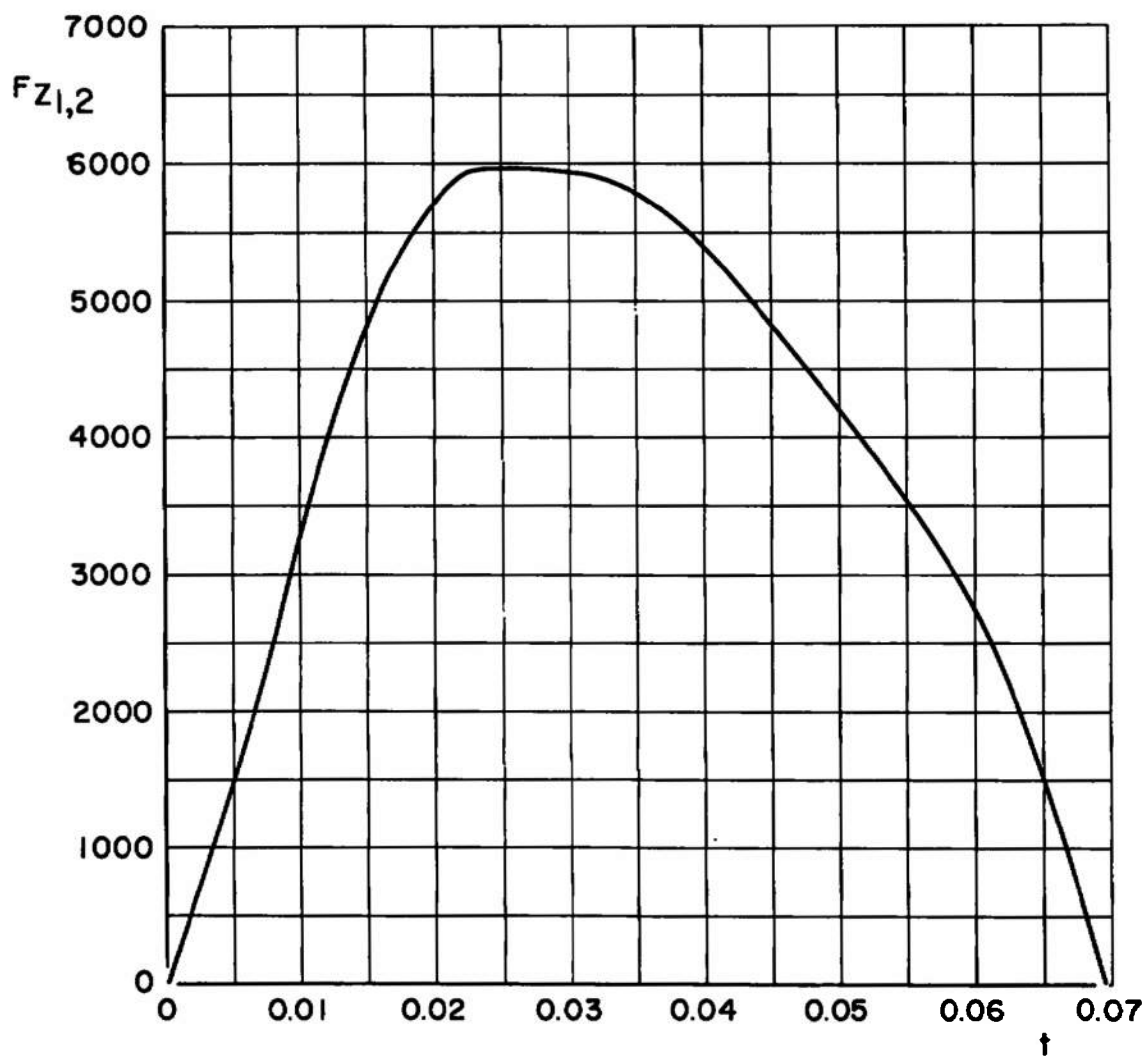
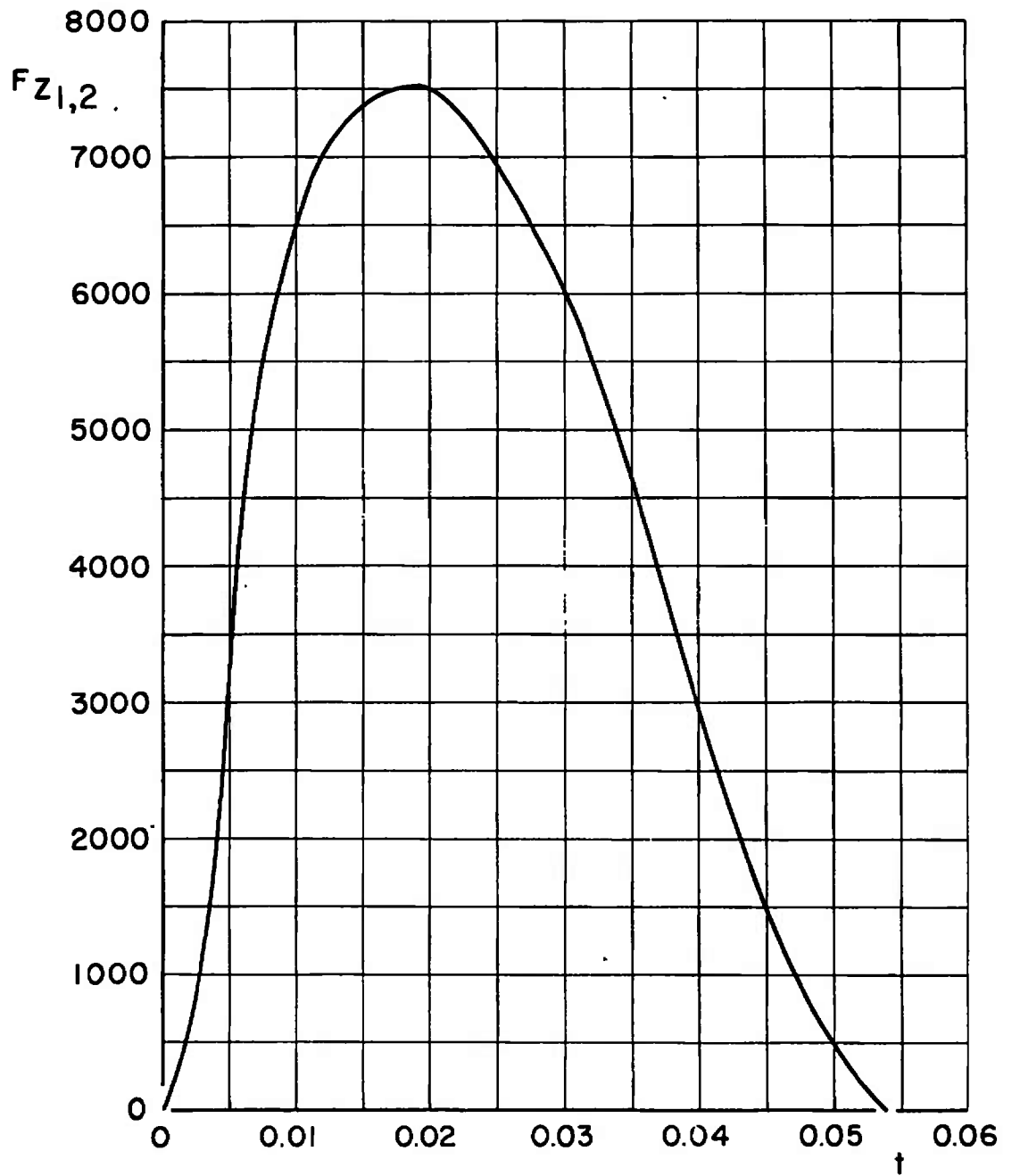


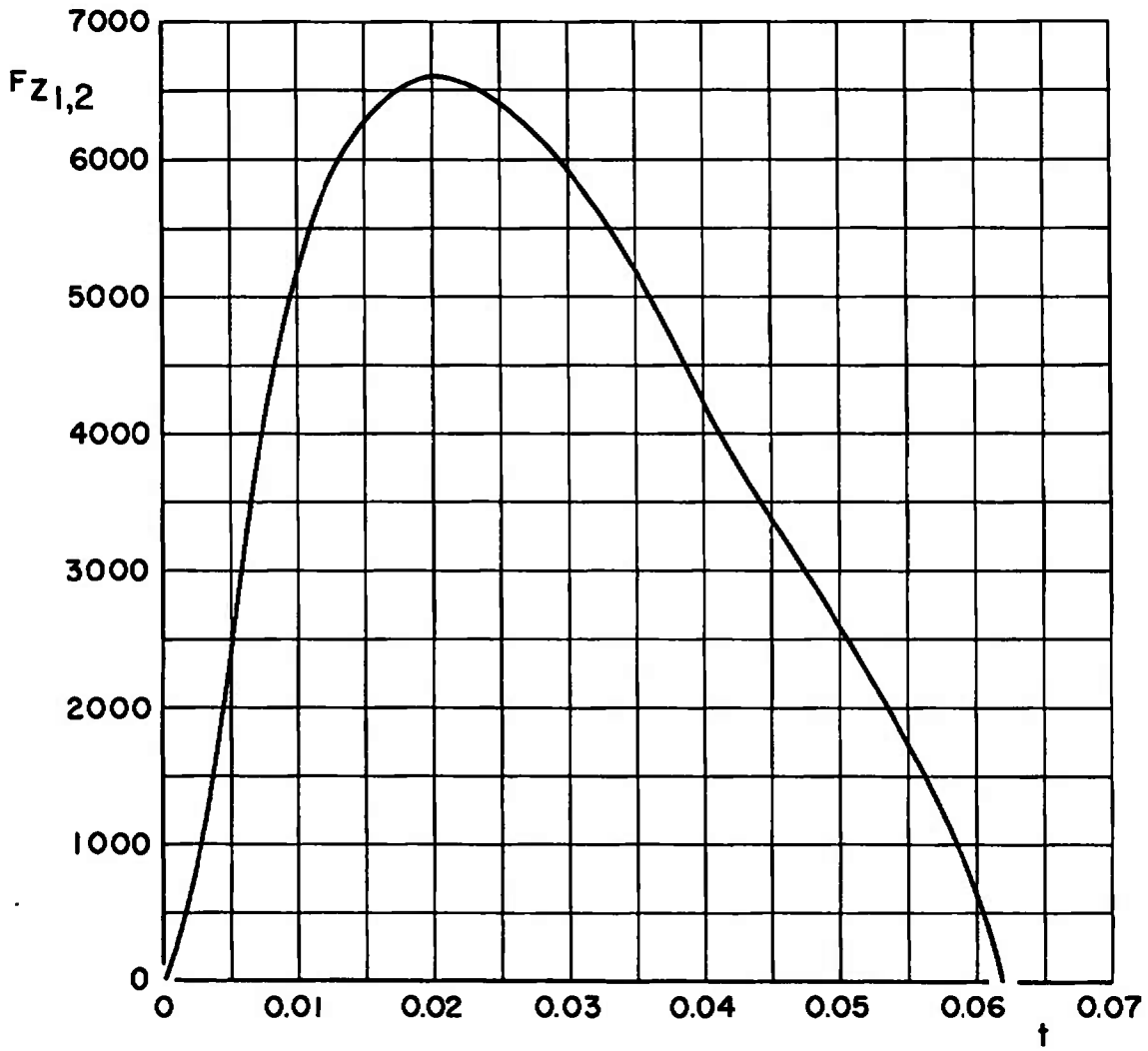
Fig. 8 Aircraft/Weapons Loading Nomenclature



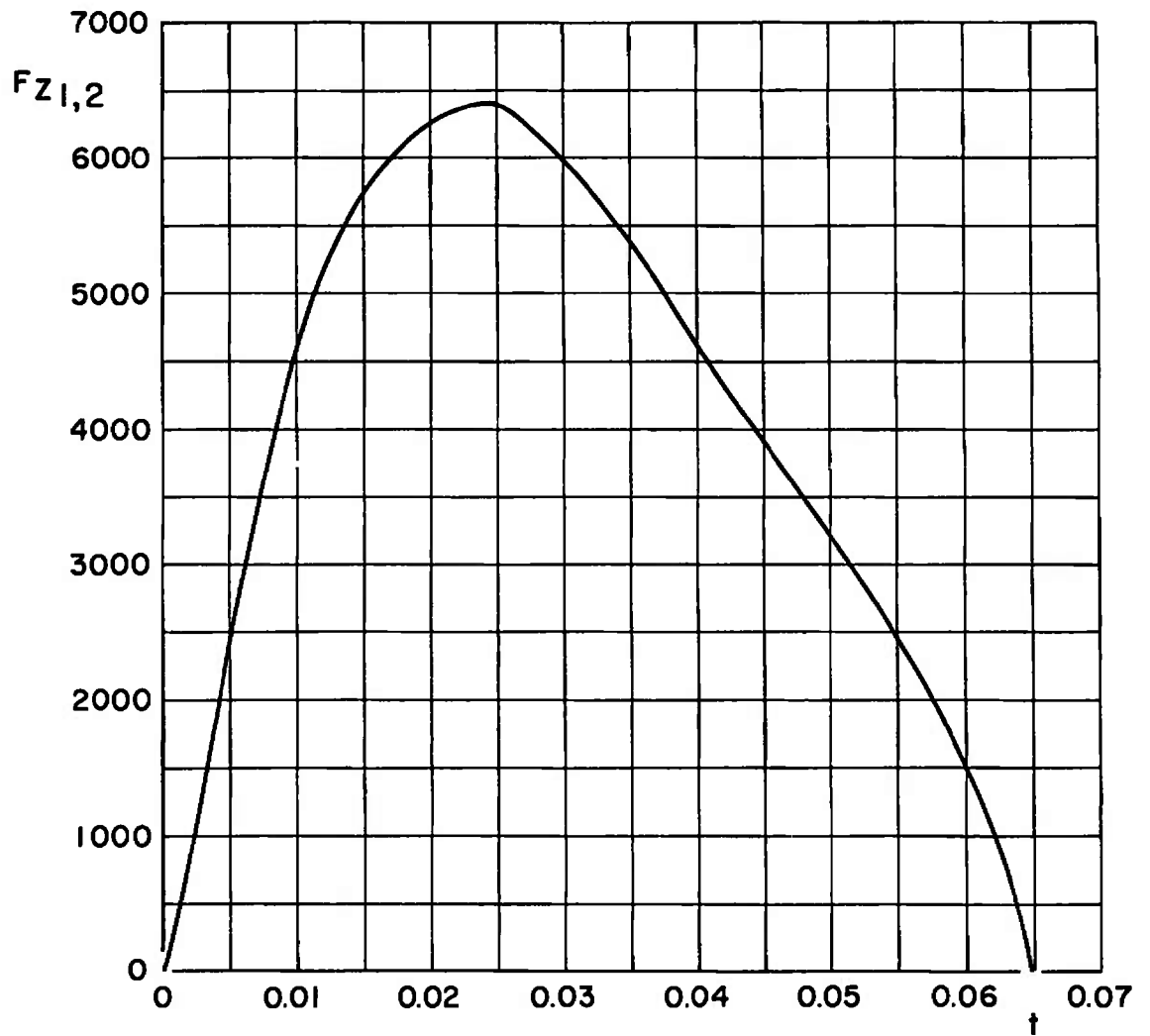
a. Configurations 1 and 4  
Fig. 9 Ejector Force Function for Inboard Pylon



b. Configurations 3 and 6  
Fig. 9 Continued

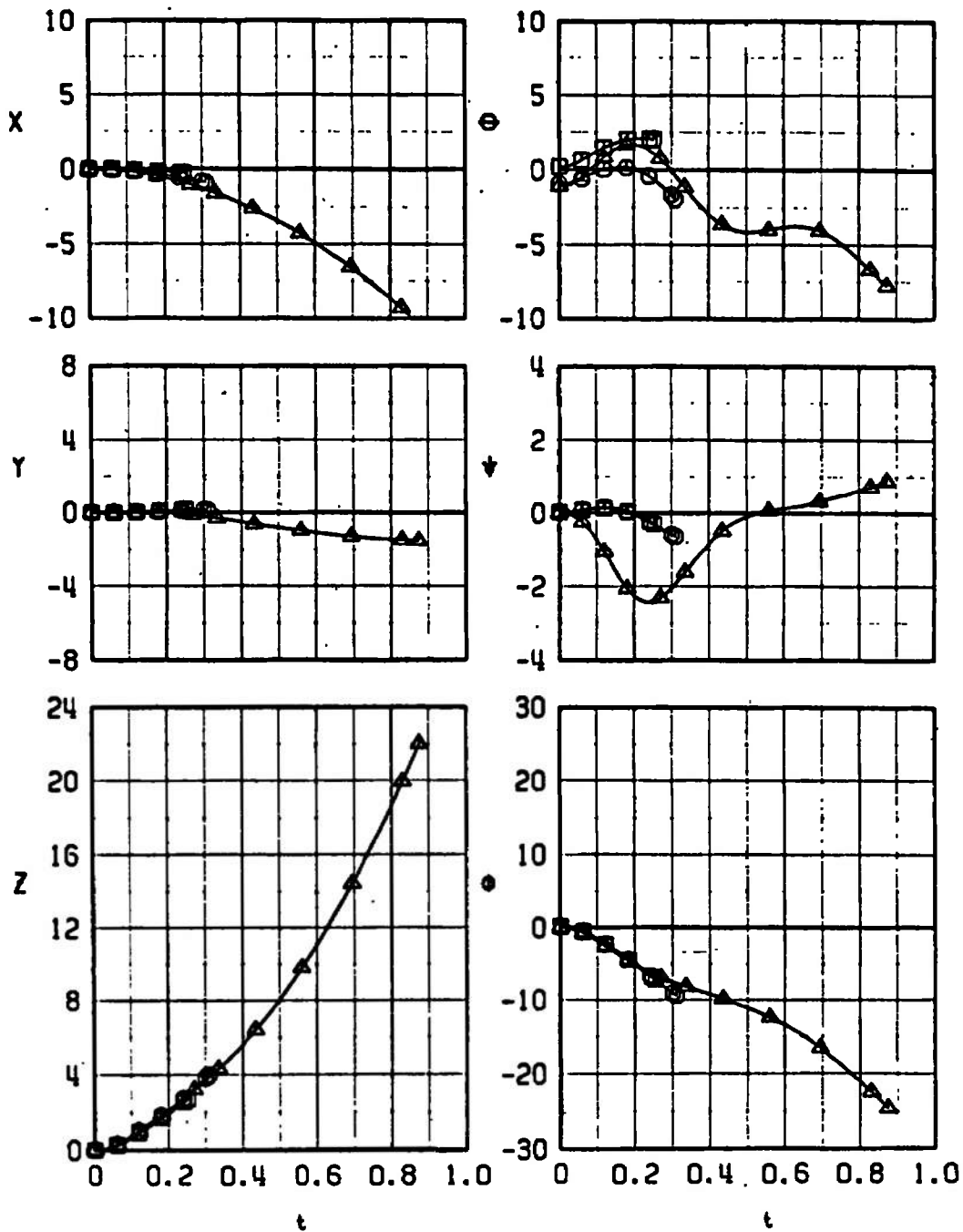


c. Configuration 2  
Fig. 9 Continued



d. Configuration 5  
Fig. 9 Concluded

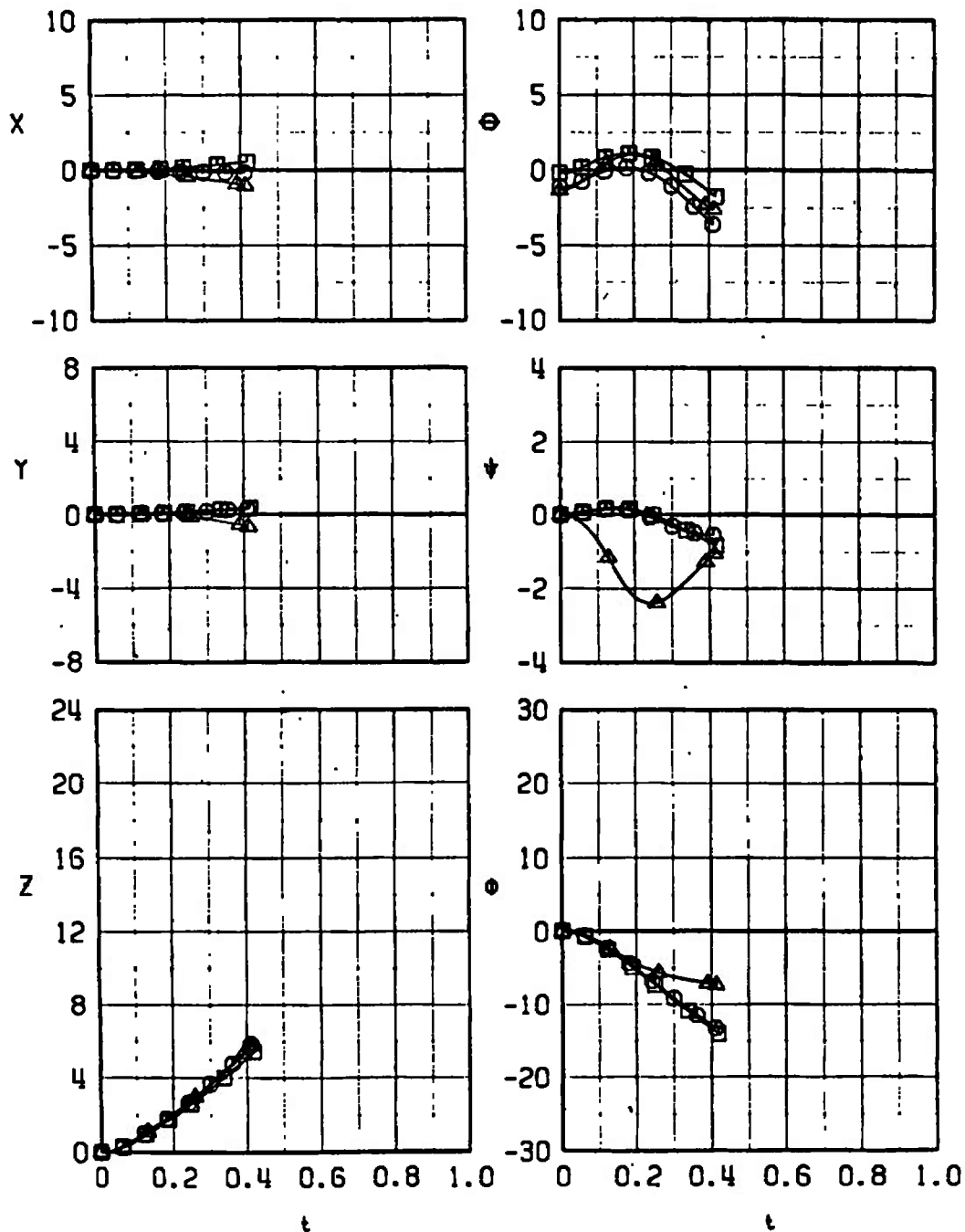
SYM	$M_\infty$	$\alpha$
□	0.70	1.2
○	0.87	0.1
△	0.95	-0.1



a. Configuration 1,  $\gamma = 0$

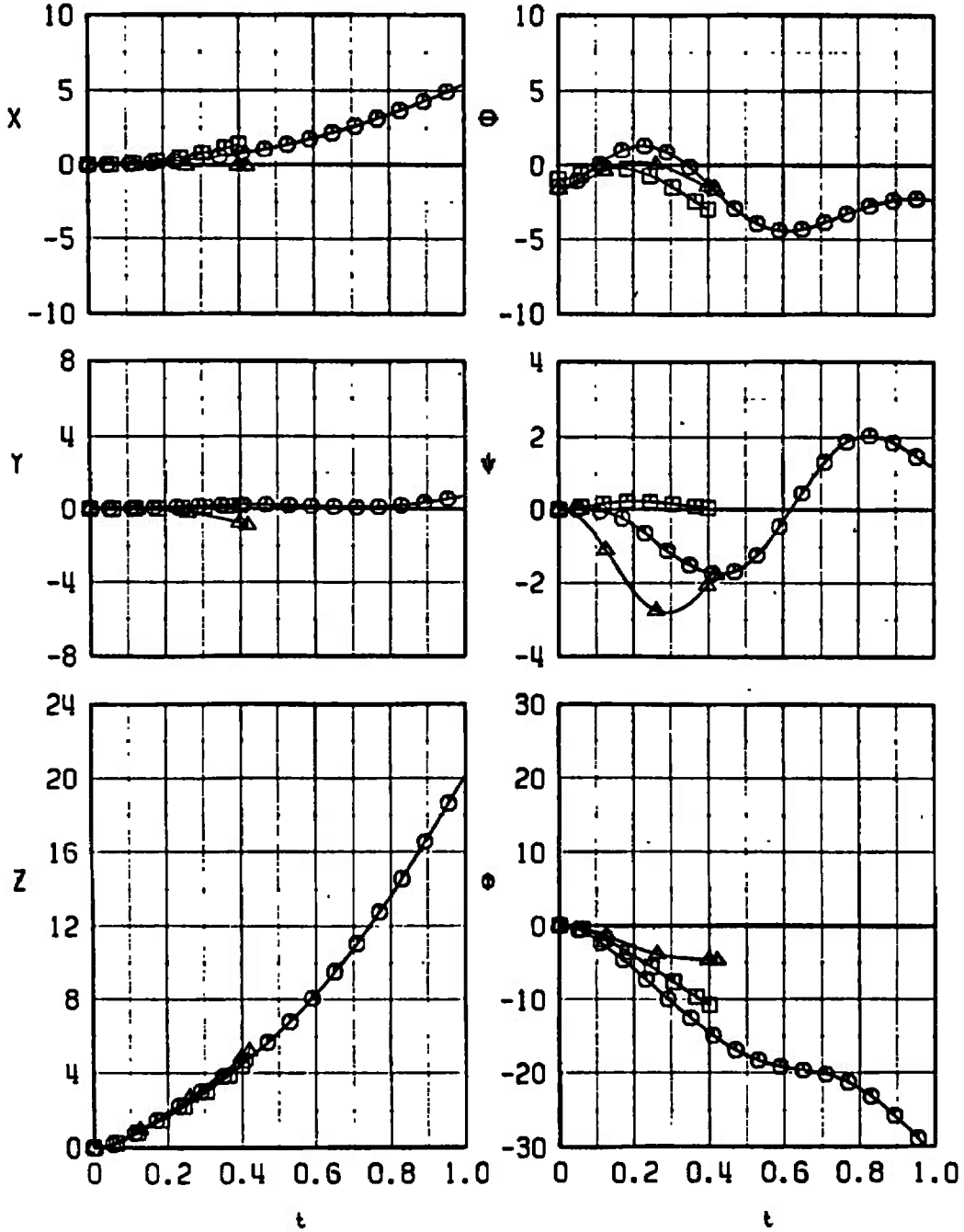
Fig. 10 Mach Number Comparison of Pave Storm I Separation Trajectories for Different Dive Angles

SYM	$M_\infty$	$\alpha$
□	0.70	0.8
○	0.87	-0.1
△	0.95	-0.3



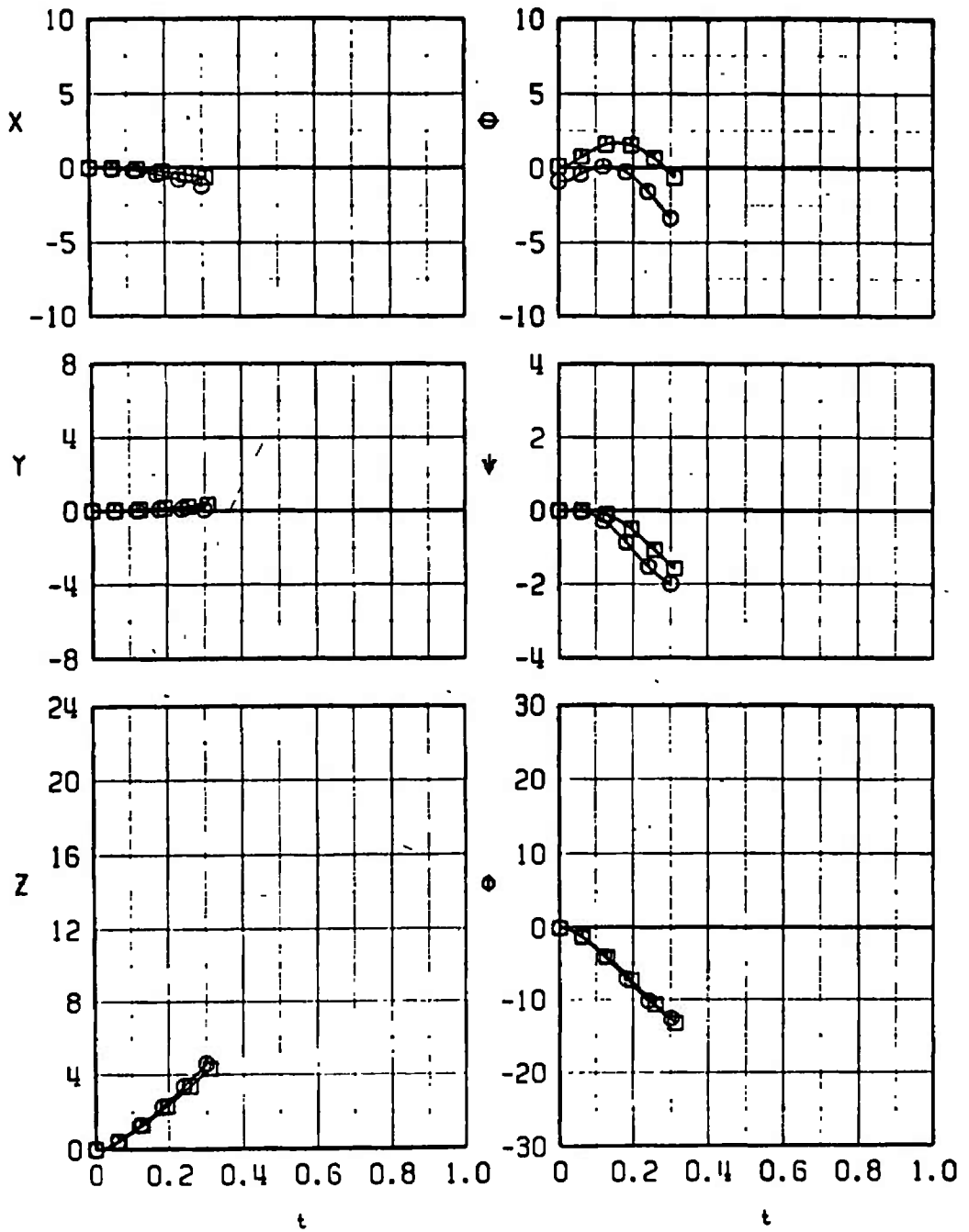
b. Configuration 1,  $\gamma = 30$   
 Fig. 10 Continued

SYM	$M_\infty$	$\alpha$
□	0.70	0.1
○	0.87	-0.4
△	0.95	-0.6



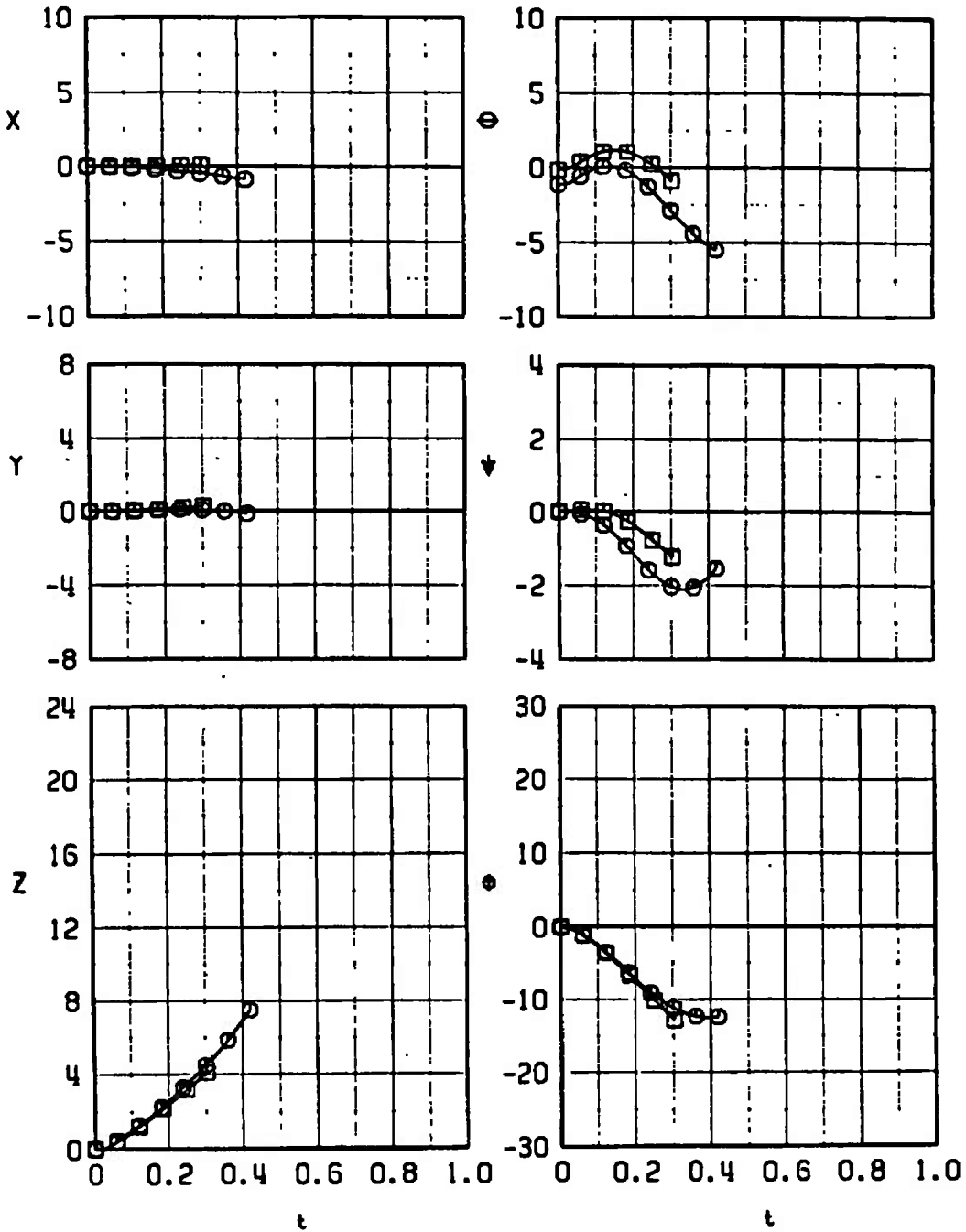
c. Configuration 1,  $\gamma = 60$   
 Fig. 10 Continued

SYM	$M_\infty$	$\alpha$
□	0.70	1.1
○	0.87	0.1



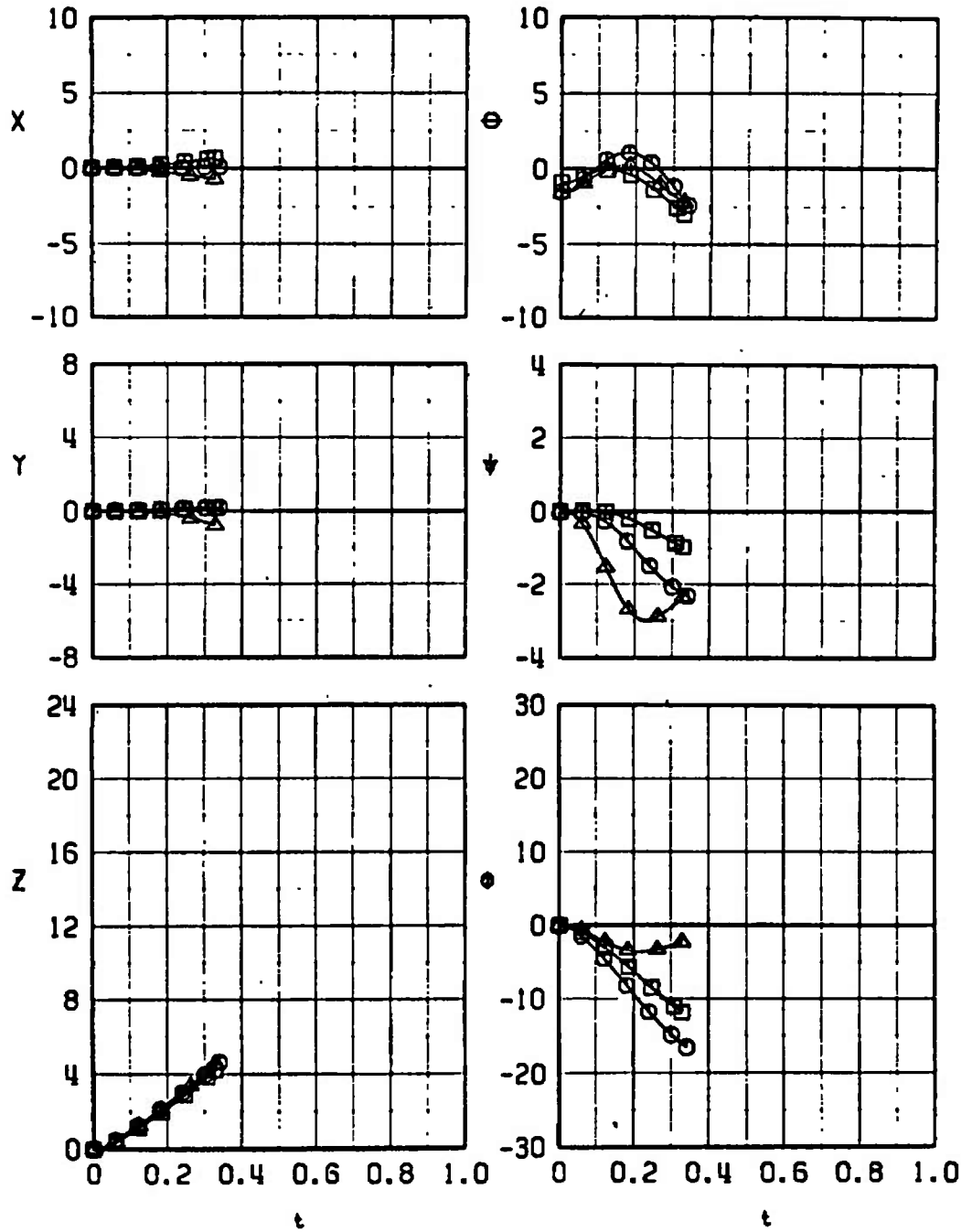
d. Configuration 2,  $\gamma = 0$   
 Fig. 10 Continued

SYM	$M_\infty$	$\alpha$
□	0.70	0.8
○	0.87	-0.1



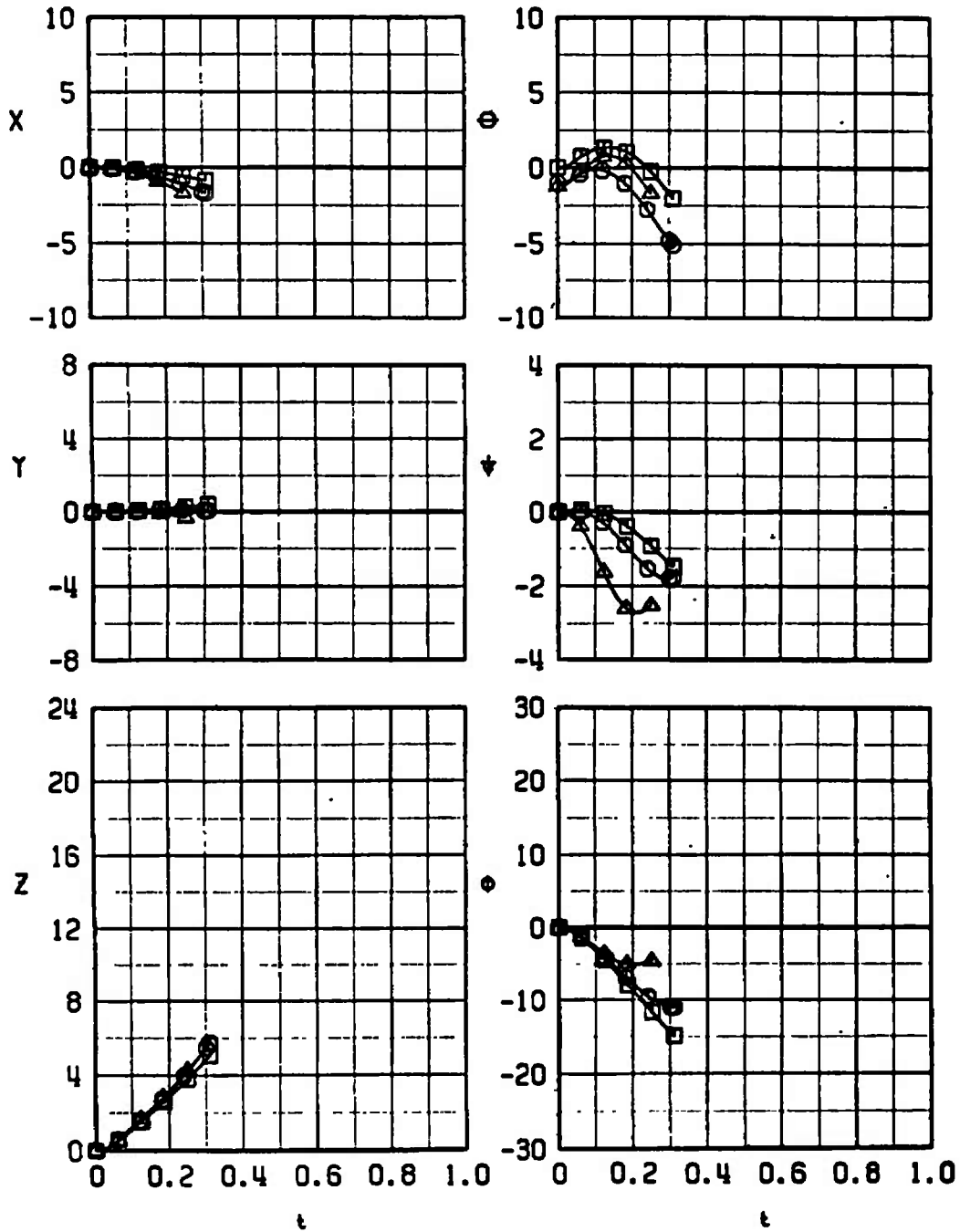
e. Configuration 2,  $\gamma = 30$   
 Fig. 10 Continued

SYM	$M_\infty$	$\alpha$
□	0.70	0.1
○	0.87	-0.5
△	0.95	-0.6



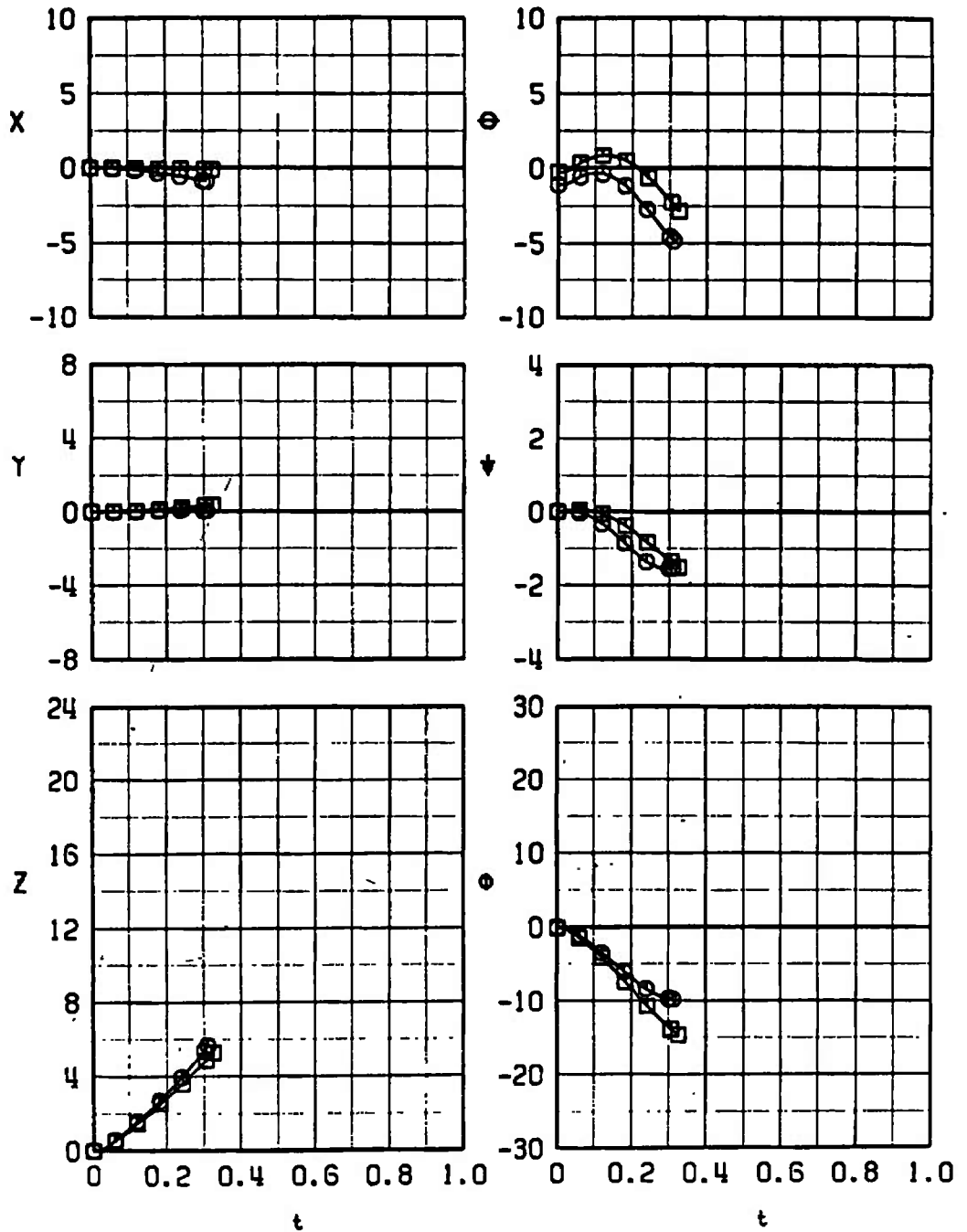
f. Configuration 2,  $\gamma = 60$   
 Fig. 10 Continued

SYM	$M_\infty$	$\alpha$
□	0.70	1.0
○	0.87	0.0
△	0.95	-0.2



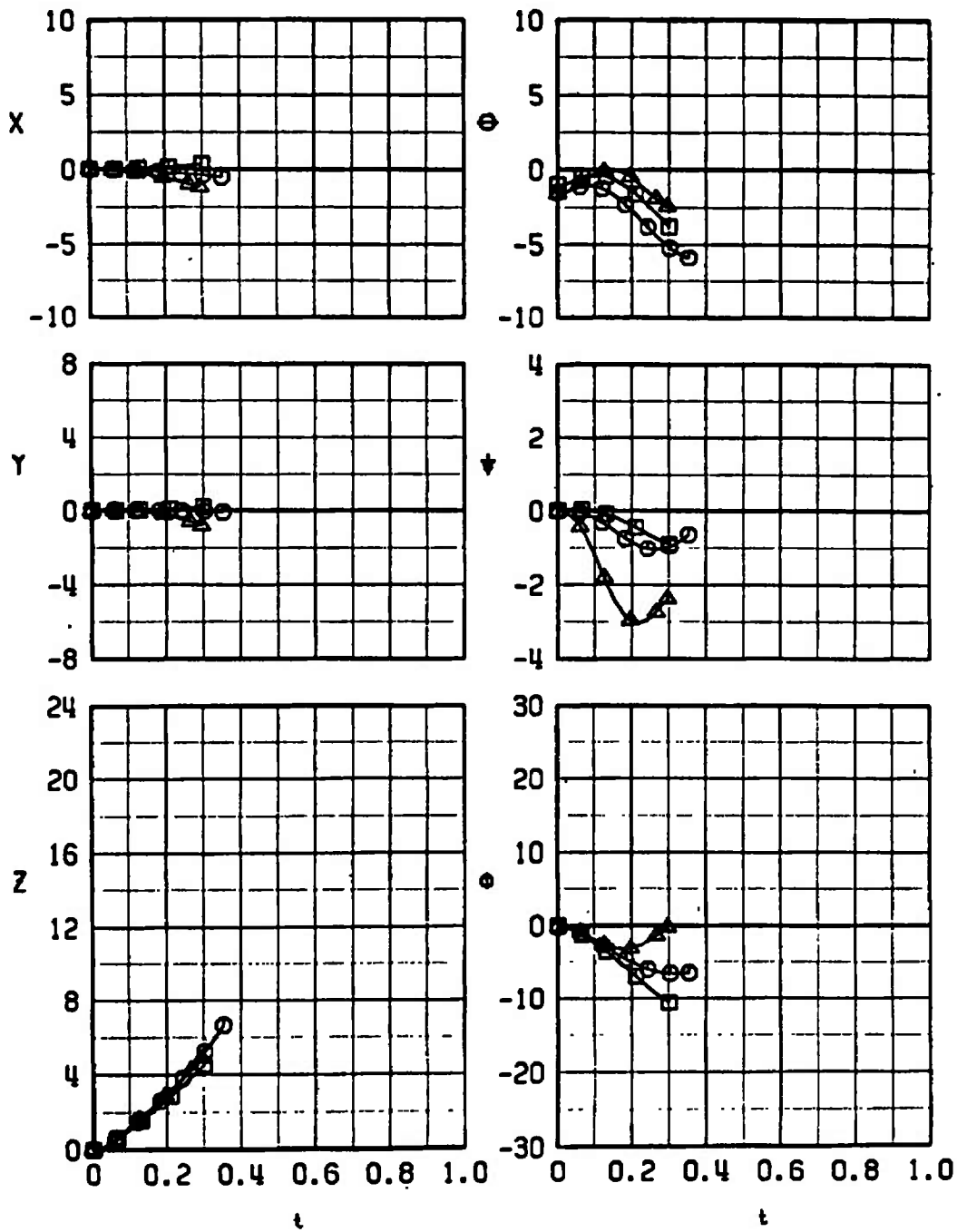
g. Configuration 3,  $\gamma = 0$   
 Fig. 10 Continued

SYM	$M_\infty$	$\alpha$
□	0.70	0.7
○	0.87	-0.1



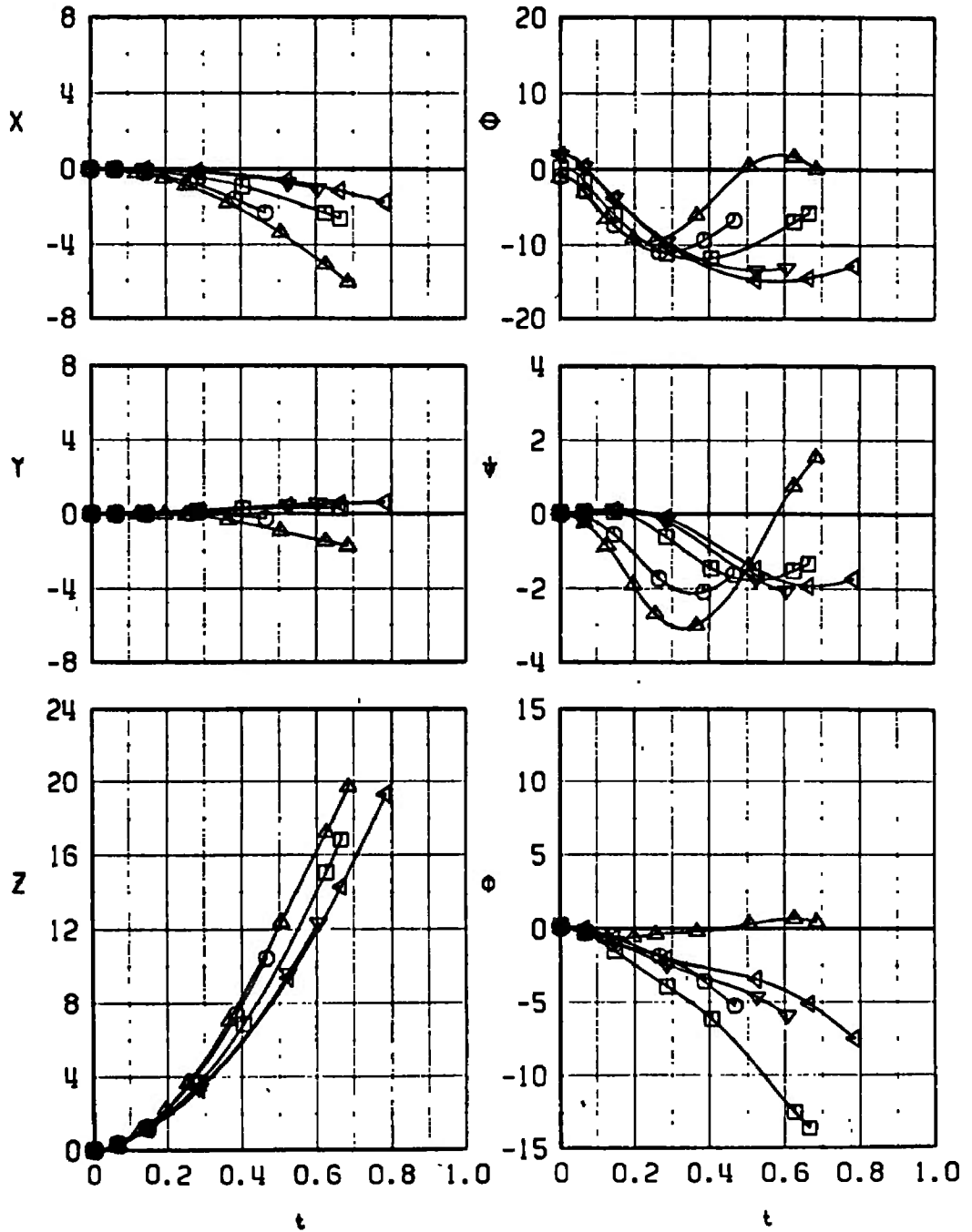
h. Configuration 3,  $\gamma = 30$   
 Fig. 10 Continued

SYM	$M_\infty$	$\alpha$
□	0.70	0.0
○	0.87	-0.5
△	0.95	



i. Configuration 3,  $\gamma = 60$   
 Fig. 10 Concluded

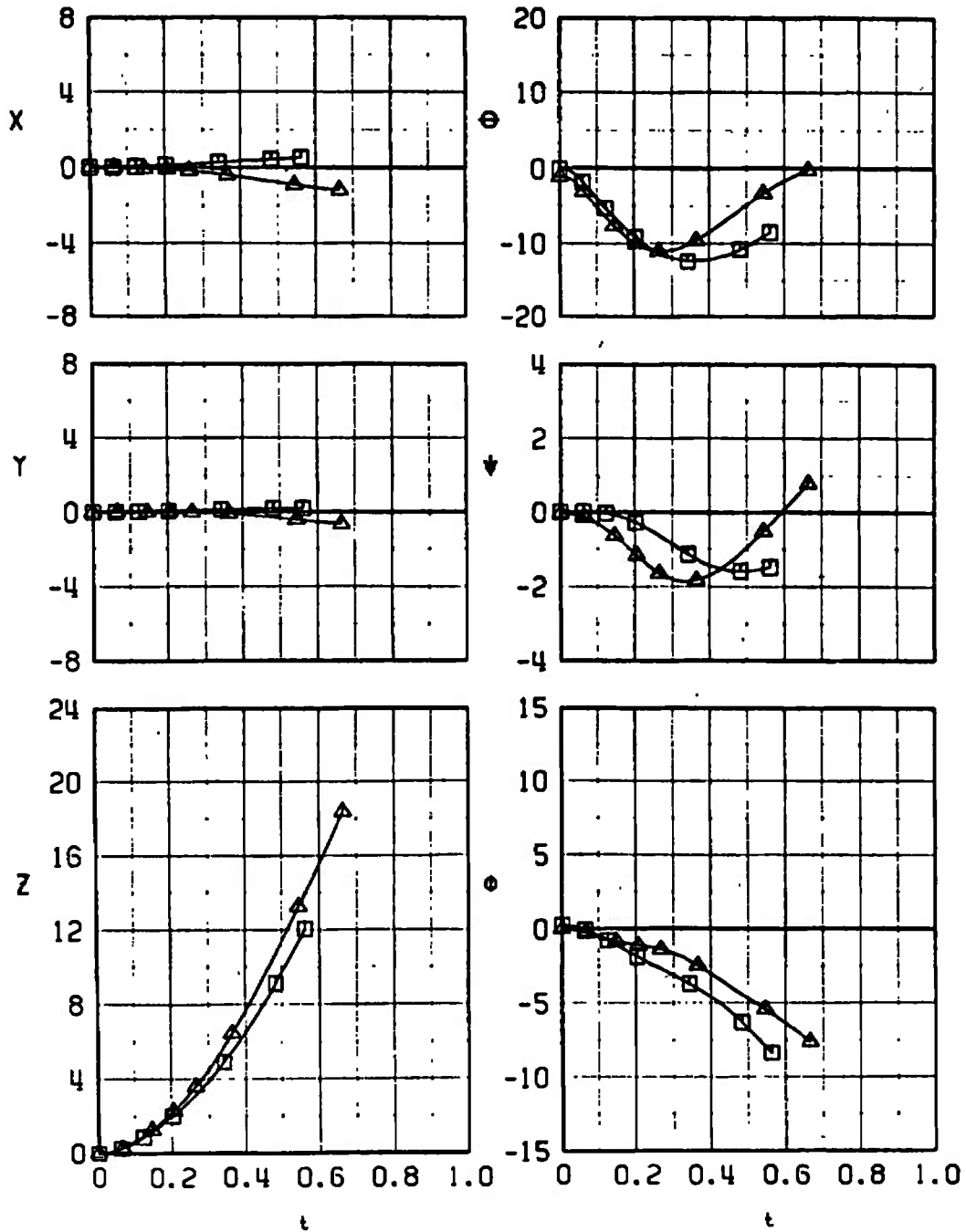
SYM	$M_\infty$	$\alpha$
$\triangleleft$	0.50	3.0
$\nabla$	0.54	3.0
$\square$	0.70	1.2
$\circ$	0.87	0.1
$\triangle$	0.95	-0.1



a. Configuration 4,  $\gamma = 0$

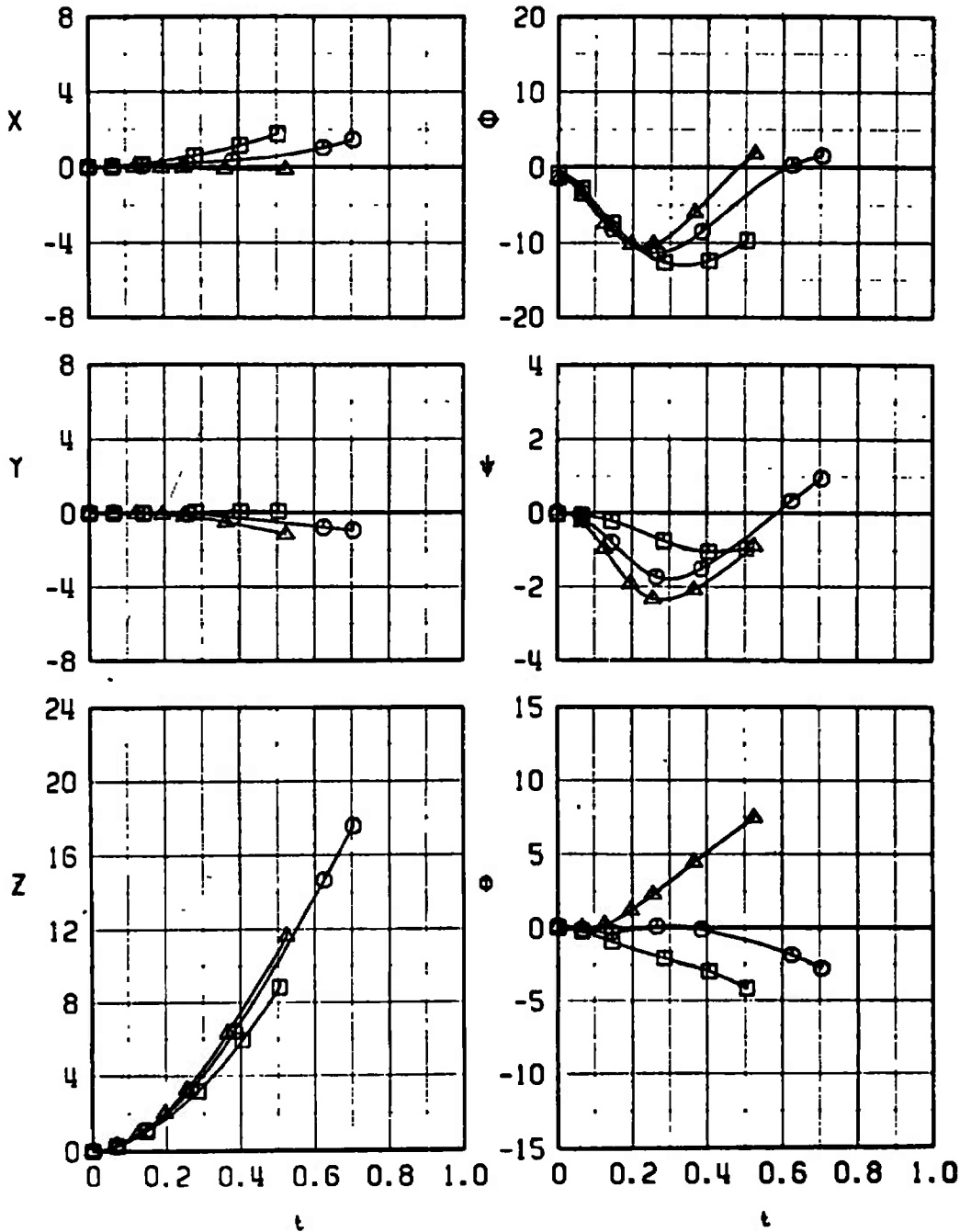
Fig. 11 Mach Number Comparison of Pave Storm II Separation Trajectories for Different Dive Angles

SYM	$M_\infty$	$\alpha$
□	0.70	0.8
△	0.87	-0.1



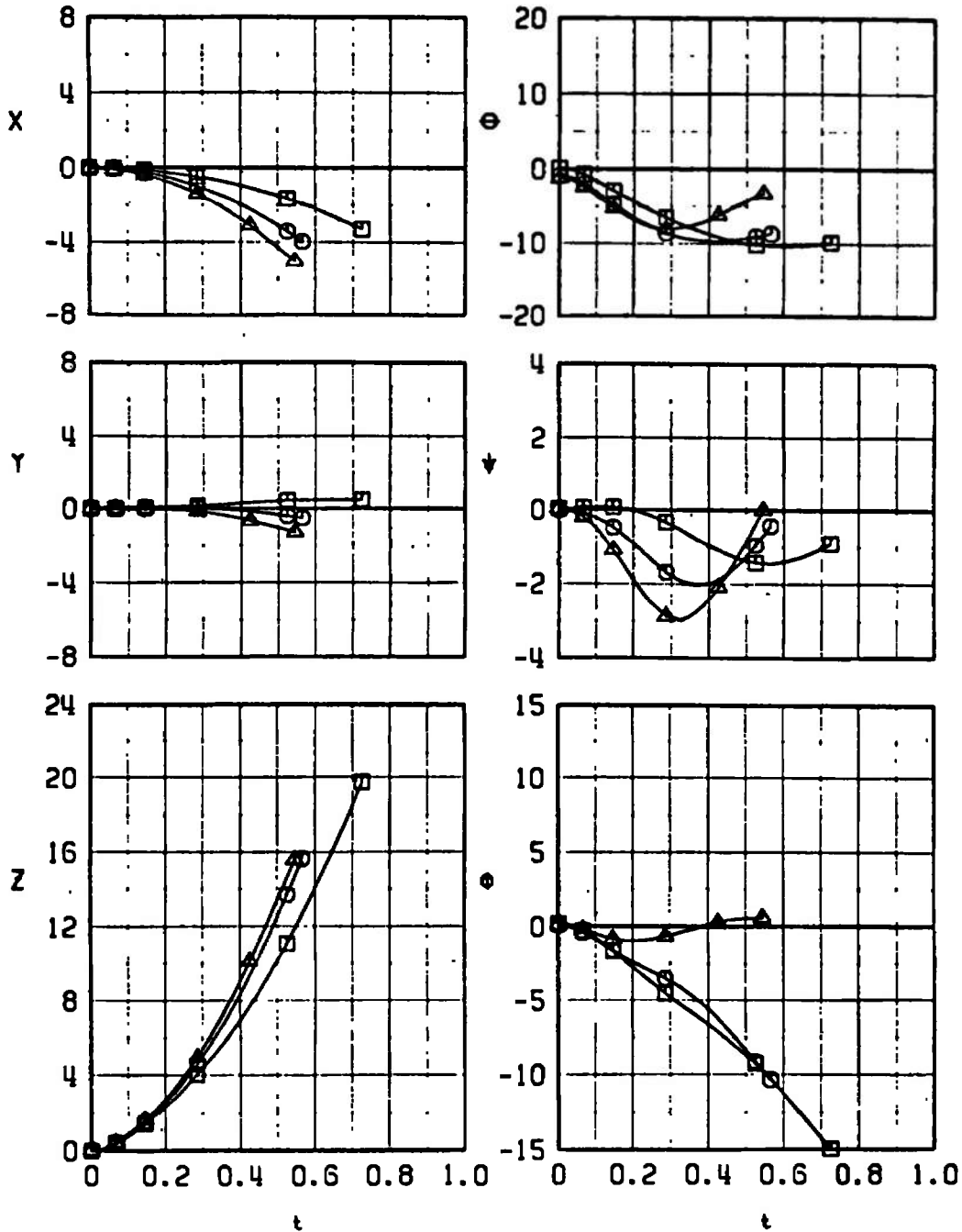
b. Configuration 4,  $\gamma = 30$   
 Fig. 11 Continued

SYM	$M_\infty$	$\alpha$
□	0.70	0.1
○	0.87	-0.4
△	0.95	-0.6



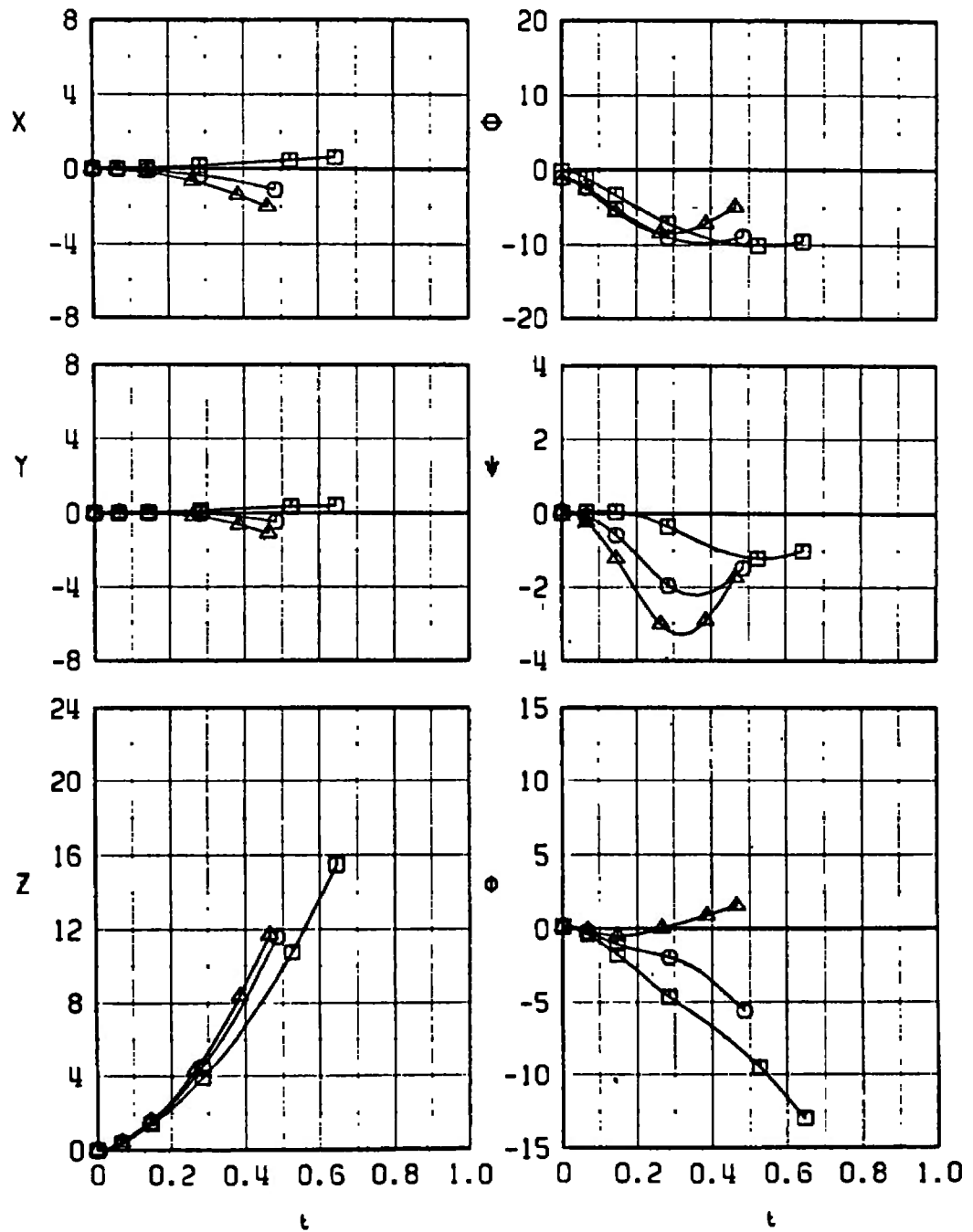
c. Configuration 4,  $\gamma = 60$   
 Fig. 11 Continued

SYM	$M_\infty$	$\alpha$
□	0.70	1.1
○	0.87	0.1
△	0.95	-0.2



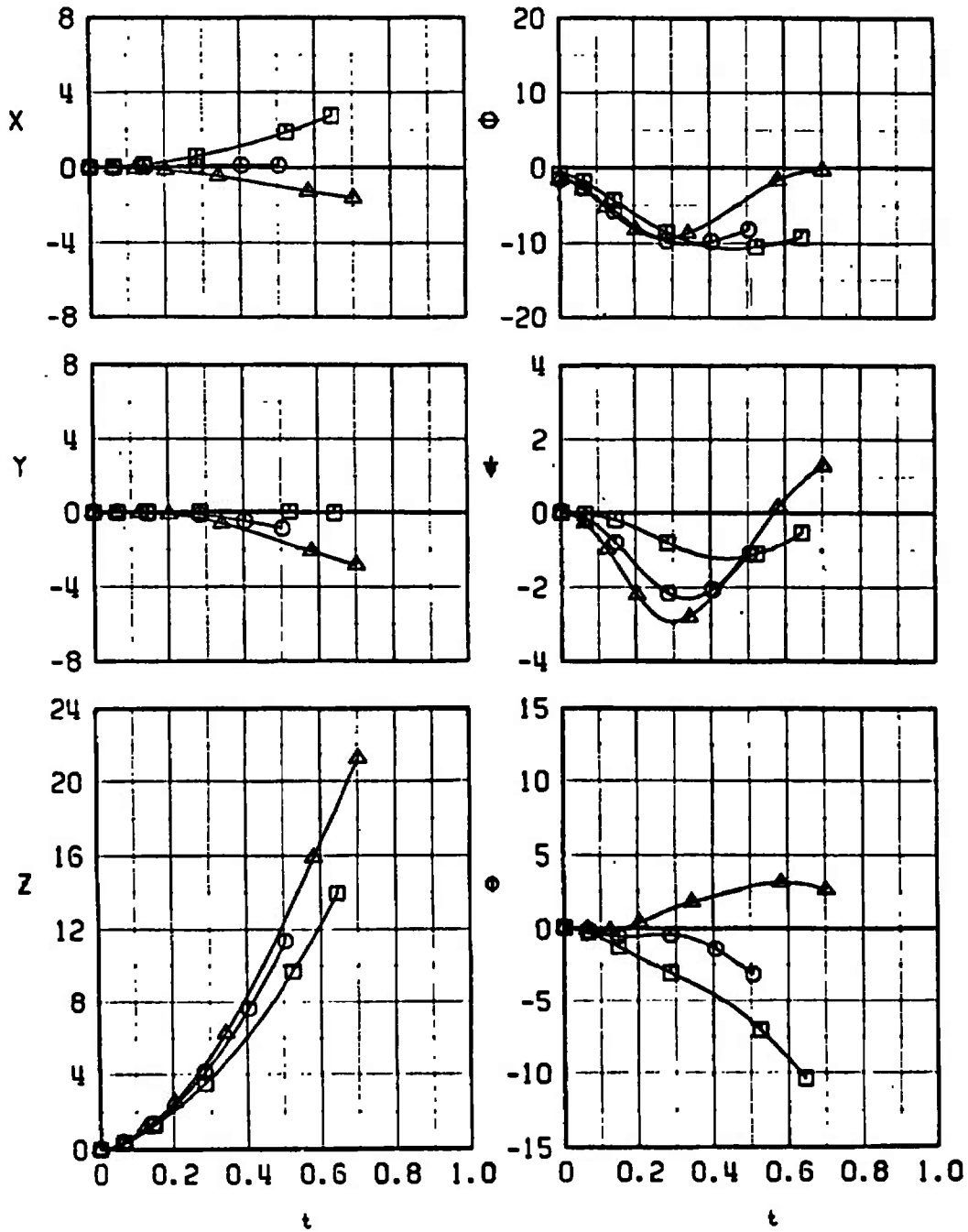
d. Configuration 5,  $\gamma = 0$   
 Fig. 11 Continued

SYM	$M_\infty$	$\alpha$
□	0.70	0.8
○	0.87	-0.1
△	0.95	-0.3



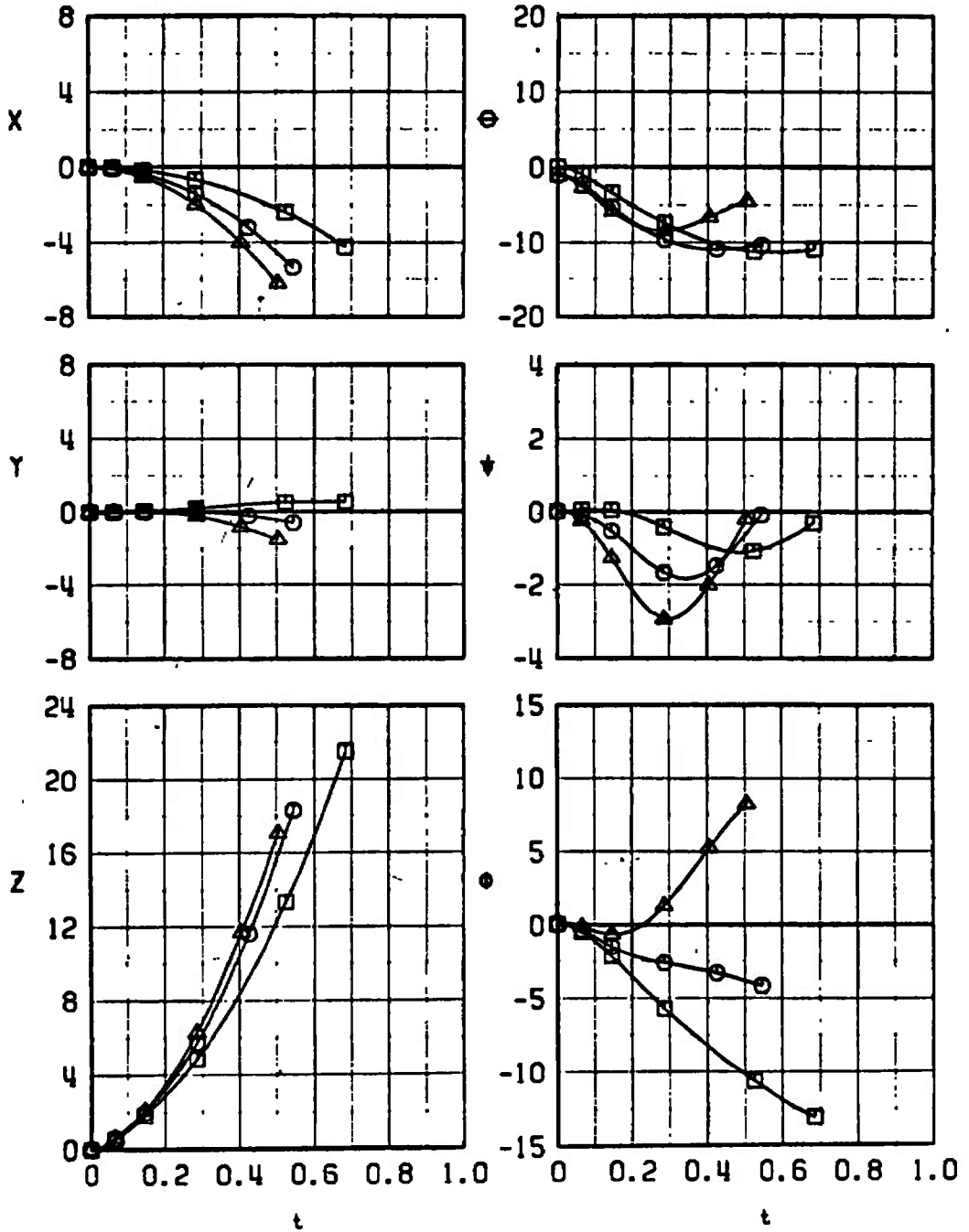
e. Configuration 5,  $\gamma = 30$   
 Fig. 11 Continued

SYM	$M_\infty$	$\alpha$
□	0.70	0.1
○	0.87	-0.5
△	0.95	-0.6



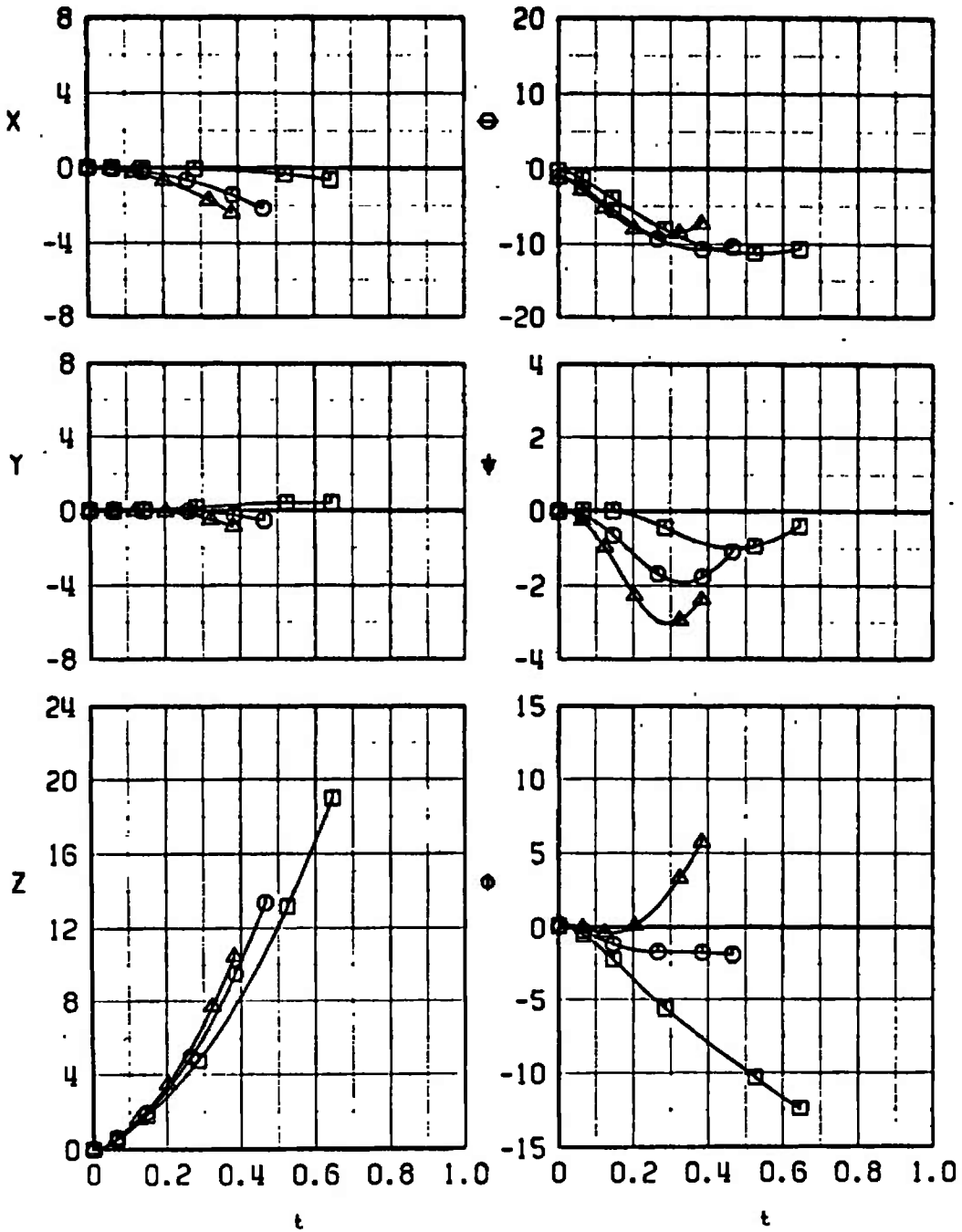
f. Configuration 5,  $\gamma = 60$   
 Fig. 11 Continued

SYM	$M_\infty$	$\alpha$
□	0.70	1.0
○	0.87	0.0
△	0.95	-0.2



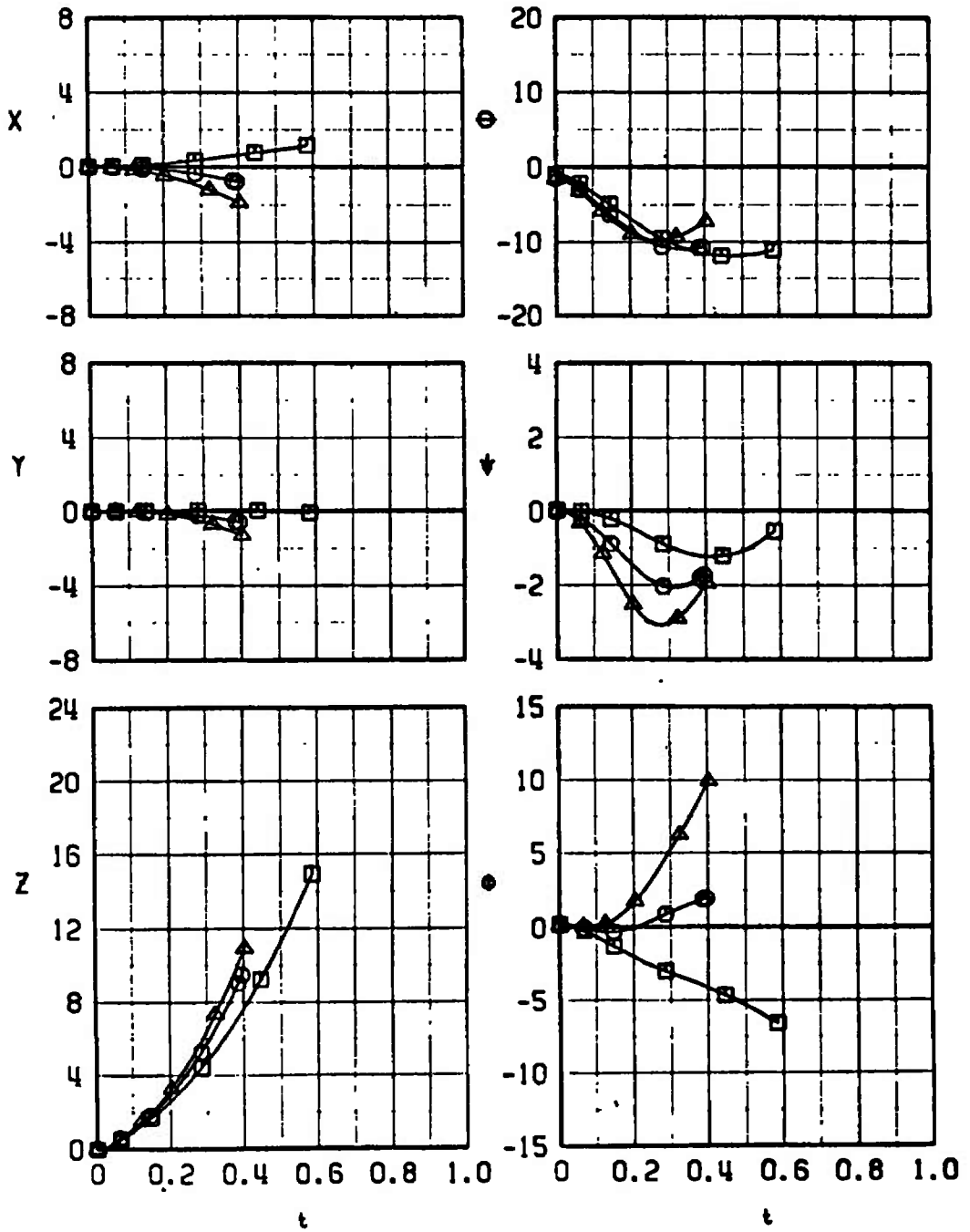
g. Configuration 6,  $\gamma = 0$   
 Fig. 11 Continued

SYM	$M_\infty$	$\alpha$
□	0.70	0.7
○	0.87	-0.1
△	0.95	-0.3



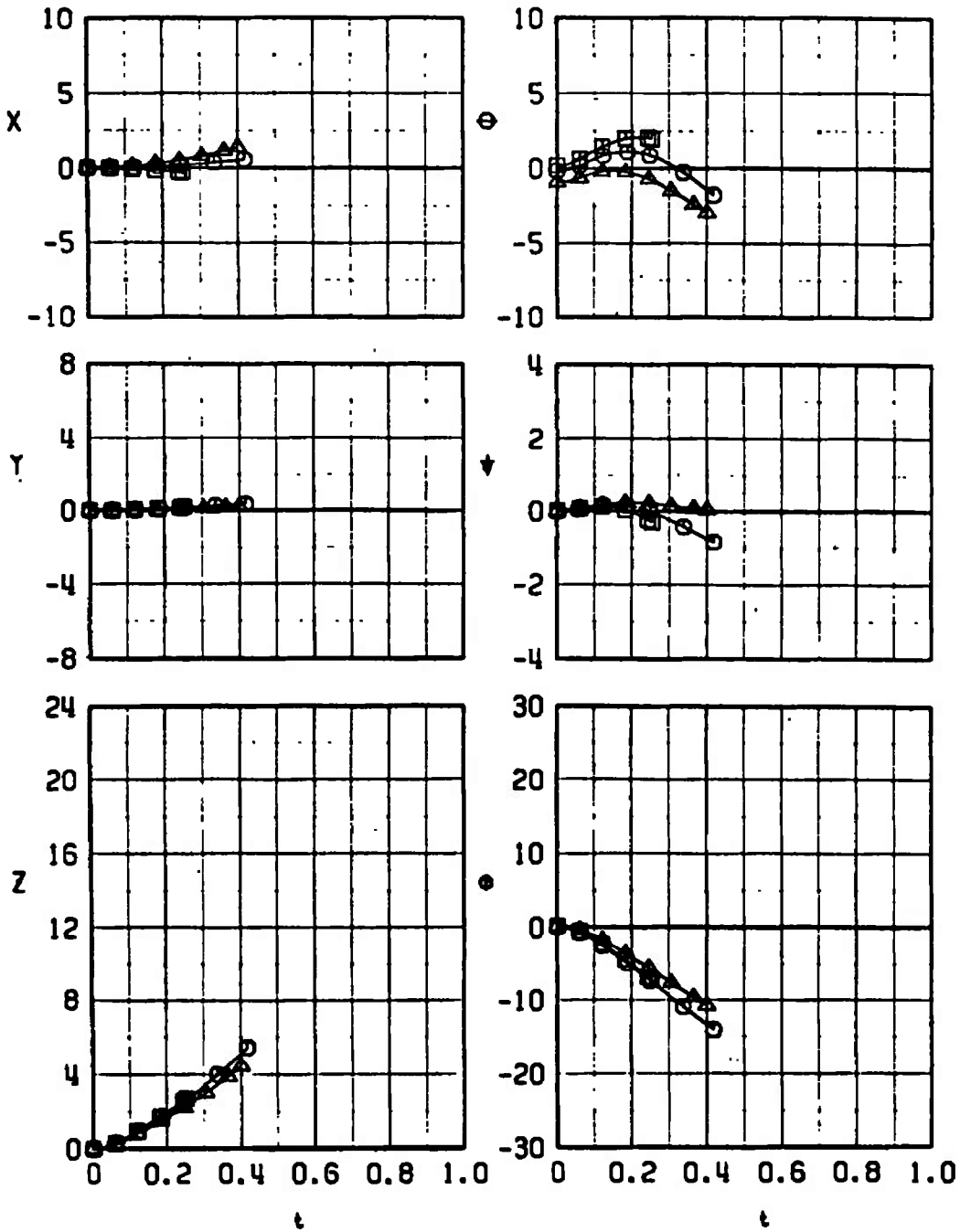
h. Configuration 6,  $\gamma = 30$   
 Fig. 11 Continued

SYM	$M_\infty$	$\alpha$
□	0.70	0.0
○	0.87	-0.5
△	0.95	-0.6



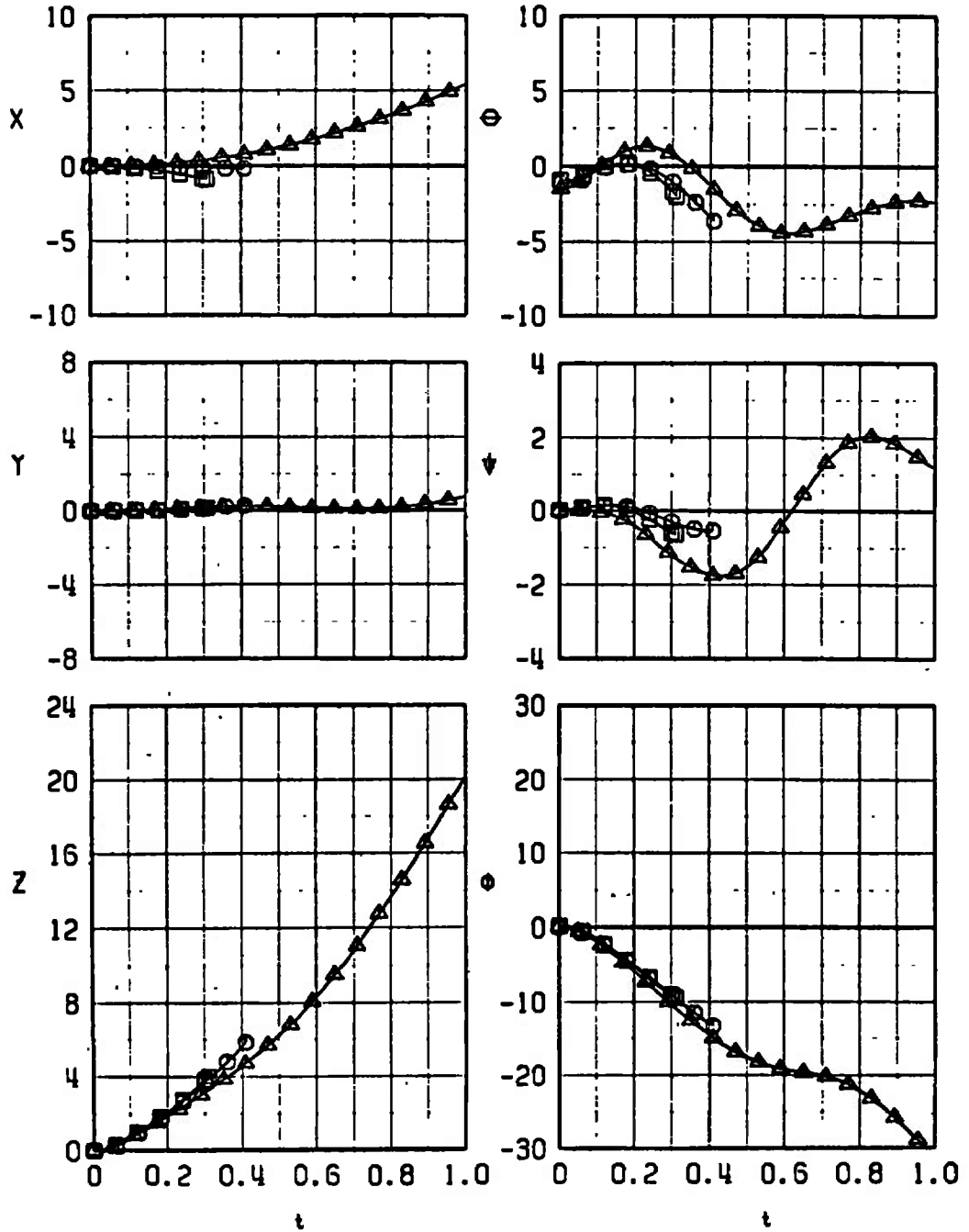
i. Configuration 6,  $\gamma = 60$   
 Fig. 11 Concluded

SYM	$\alpha$	$\gamma$
□	1.2	0
○	0.8	30
△	0.1	60



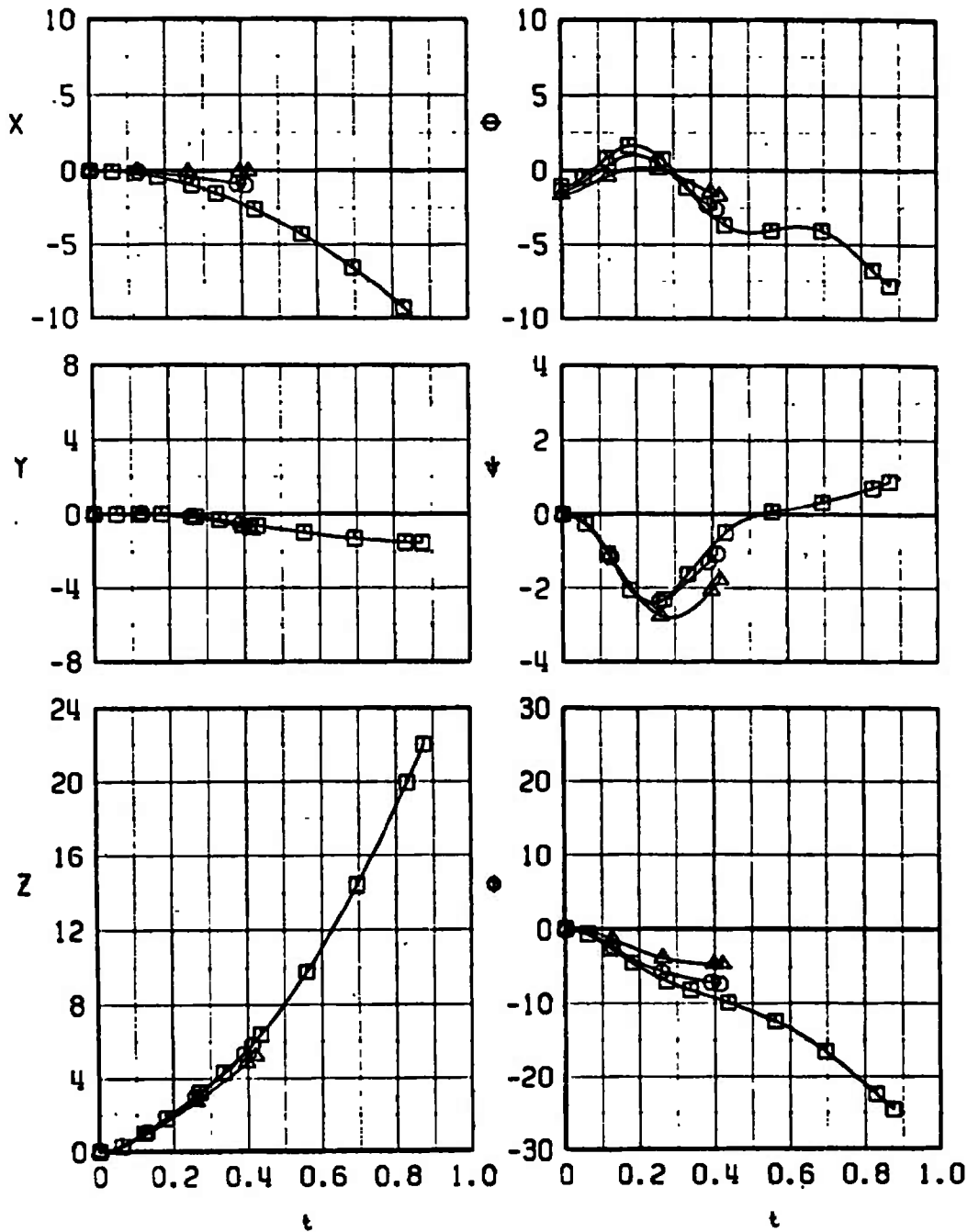
a. Configuration 1,  $M_\infty = 0.70$   
 Fig. 12 Dive Angle Comparison of Separation Trajectories

SYM	$\alpha$	$\gamma$
□	0.1	0
○	-0.1	30
△	-0.4	60



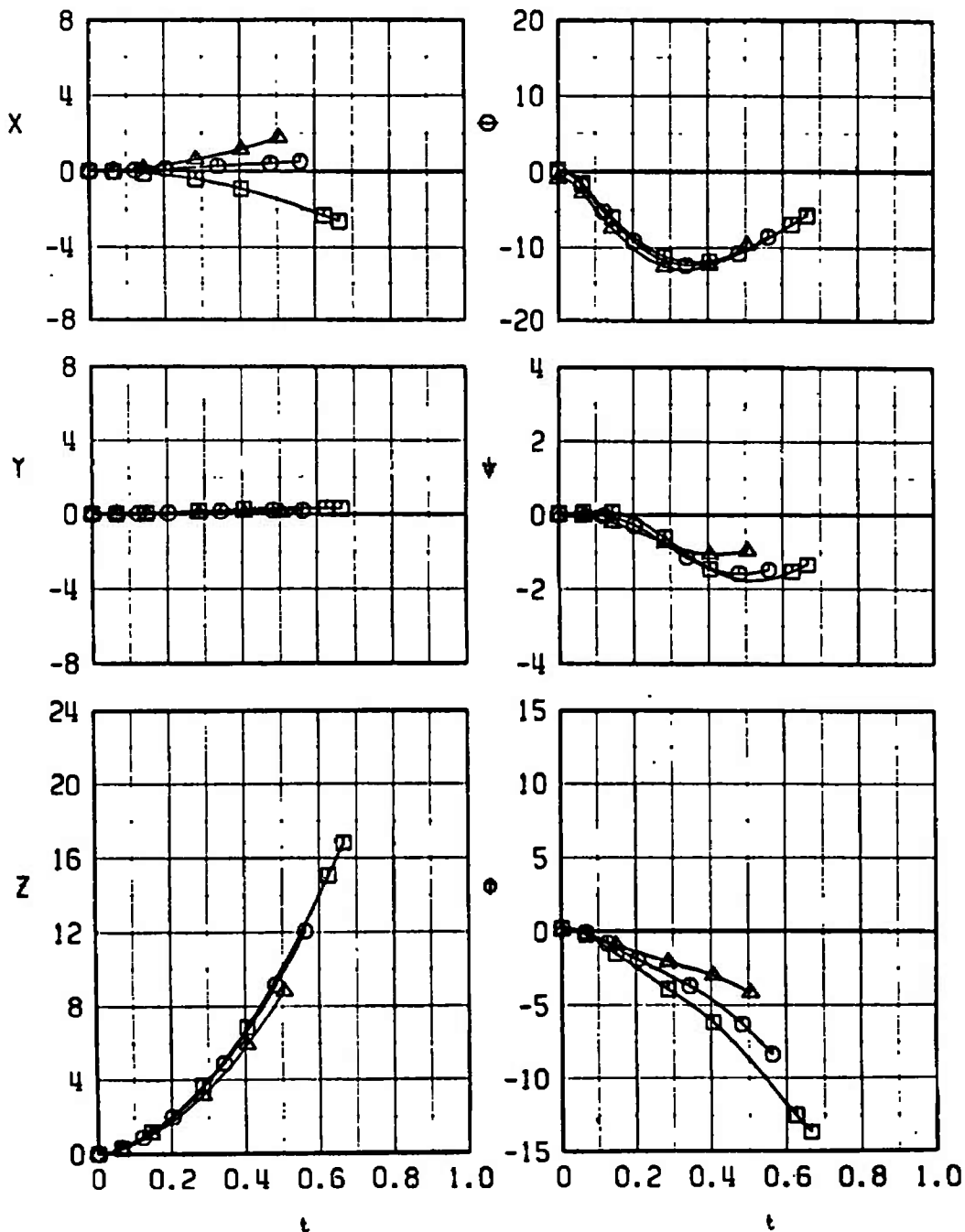
b. Configuration 1,  $M_\infty = 0.87$   
 Fig. 12 Continued

SYM	$\alpha$	$\gamma$
□	-0.1	0
○	-0.3	30
△	-0.6	60



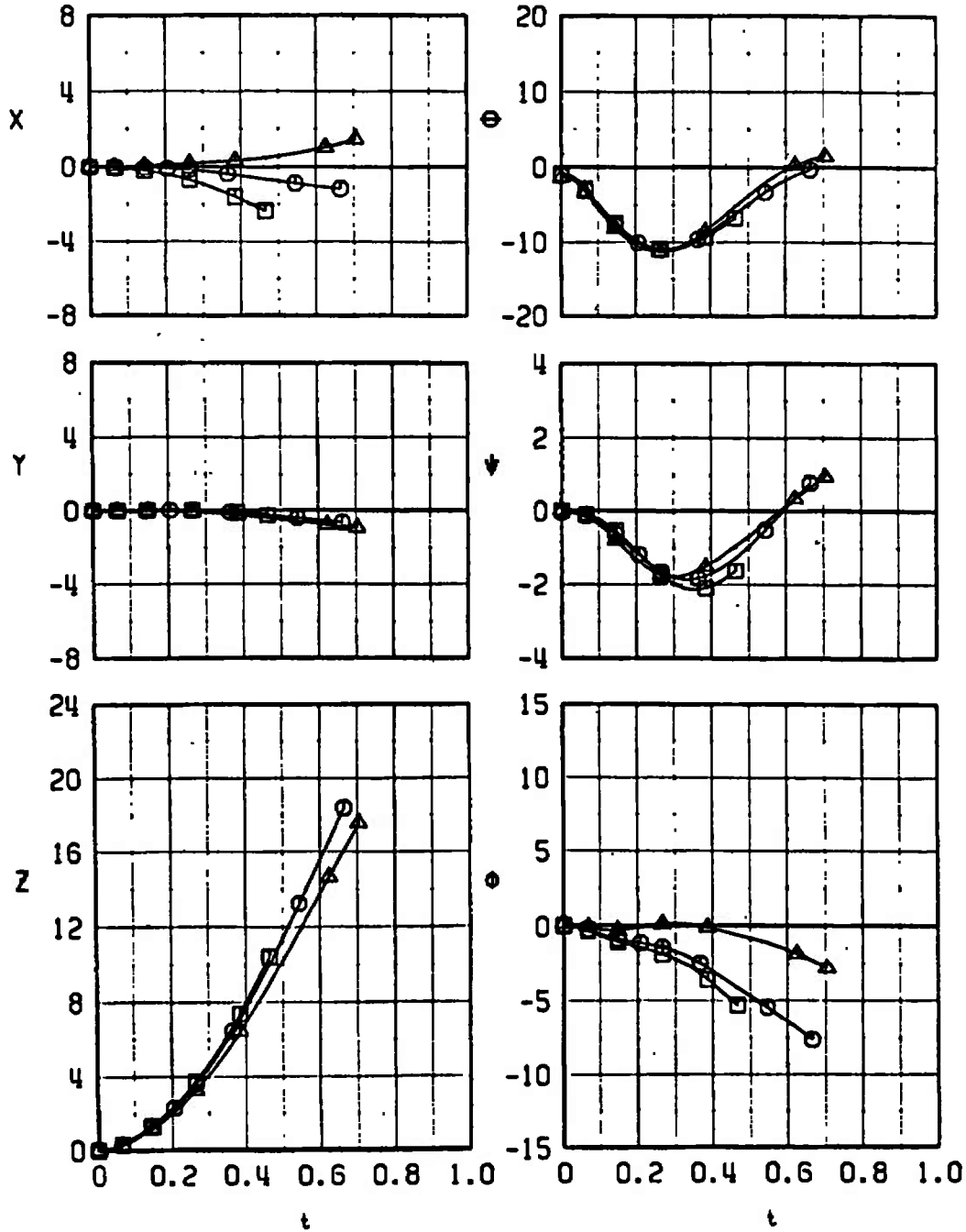
c. Configuration 1,  $M_\infty = 0.95$   
 Fig. 12 Continued

SYM	$\alpha$	$\gamma$
□	1.2	0
○	0.8	30
△	0.1	60



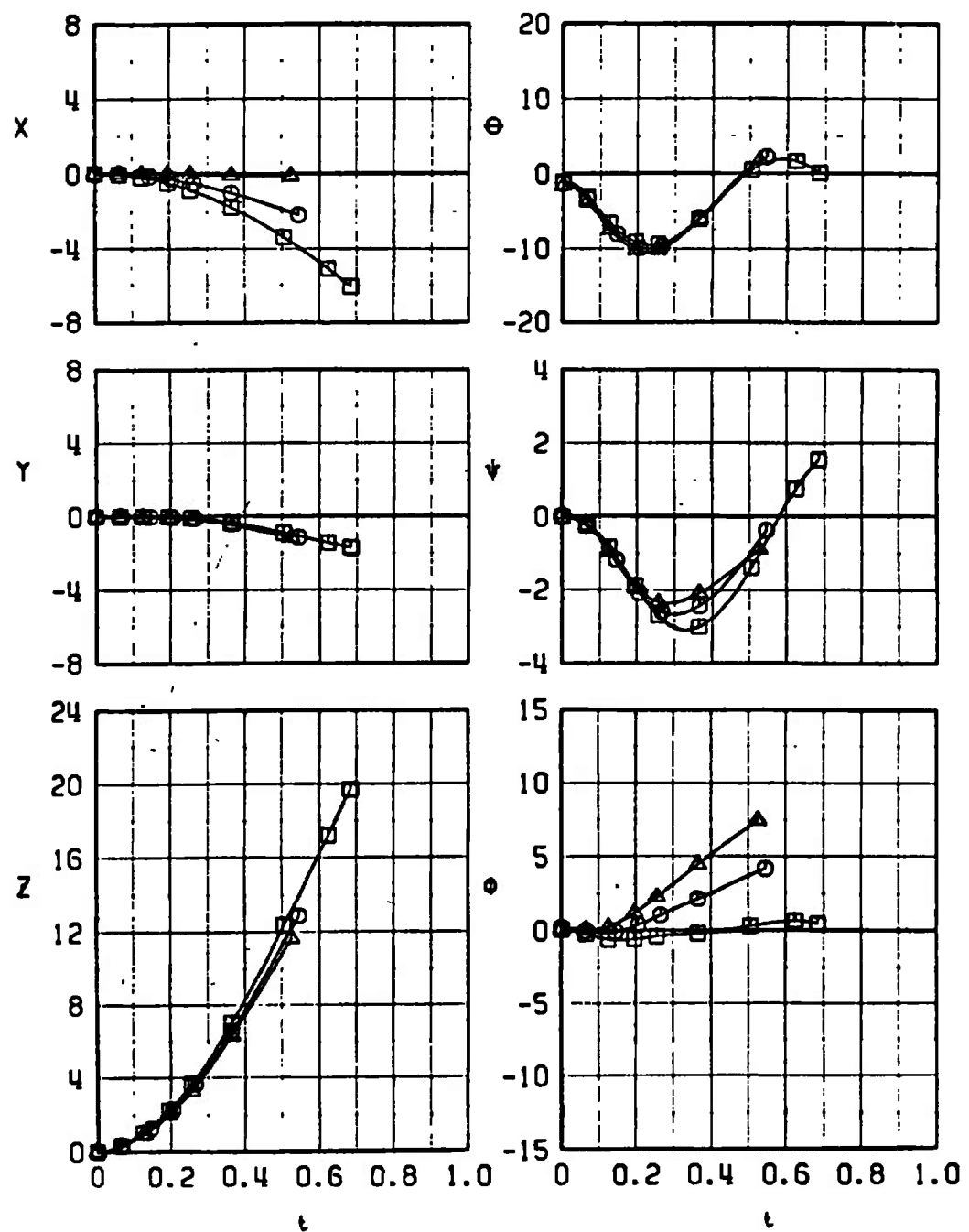
d. Configuration 4,  $M_\infty = 0.70$   
 Fig. 12 Continued

SYM	$\alpha$	$\gamma$
□	0.1	0
○	-0.1	30
△	-0.4	60



e. Configuration 4,  $M_\infty = 0.87$   
 Fig. 12 Continued

SYM	$\alpha$	$\gamma$
□	-0.1	0
○	-0.3	30
△	-0.6	60



f. Configuration 4,  $M_\infty = 0.95$   
 Fig. 12 Concluded

SYM	CONF	$\alpha$	$\bar{m}$	$X_{cg}$
□	1	-0.6	70.37	8.928
○	2	-0.6	48.30	8.897
△	3	-0.6	36.68	8.897

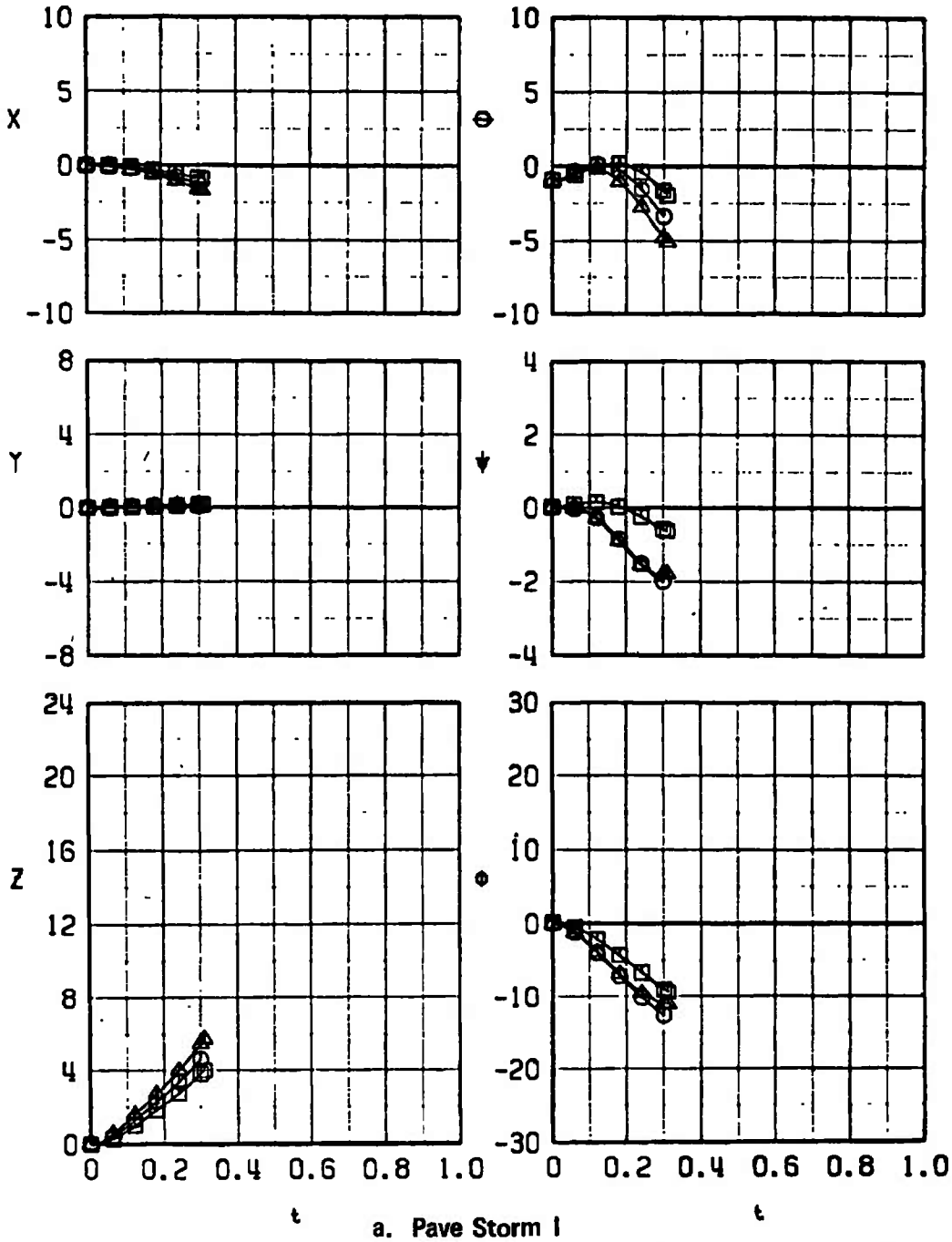
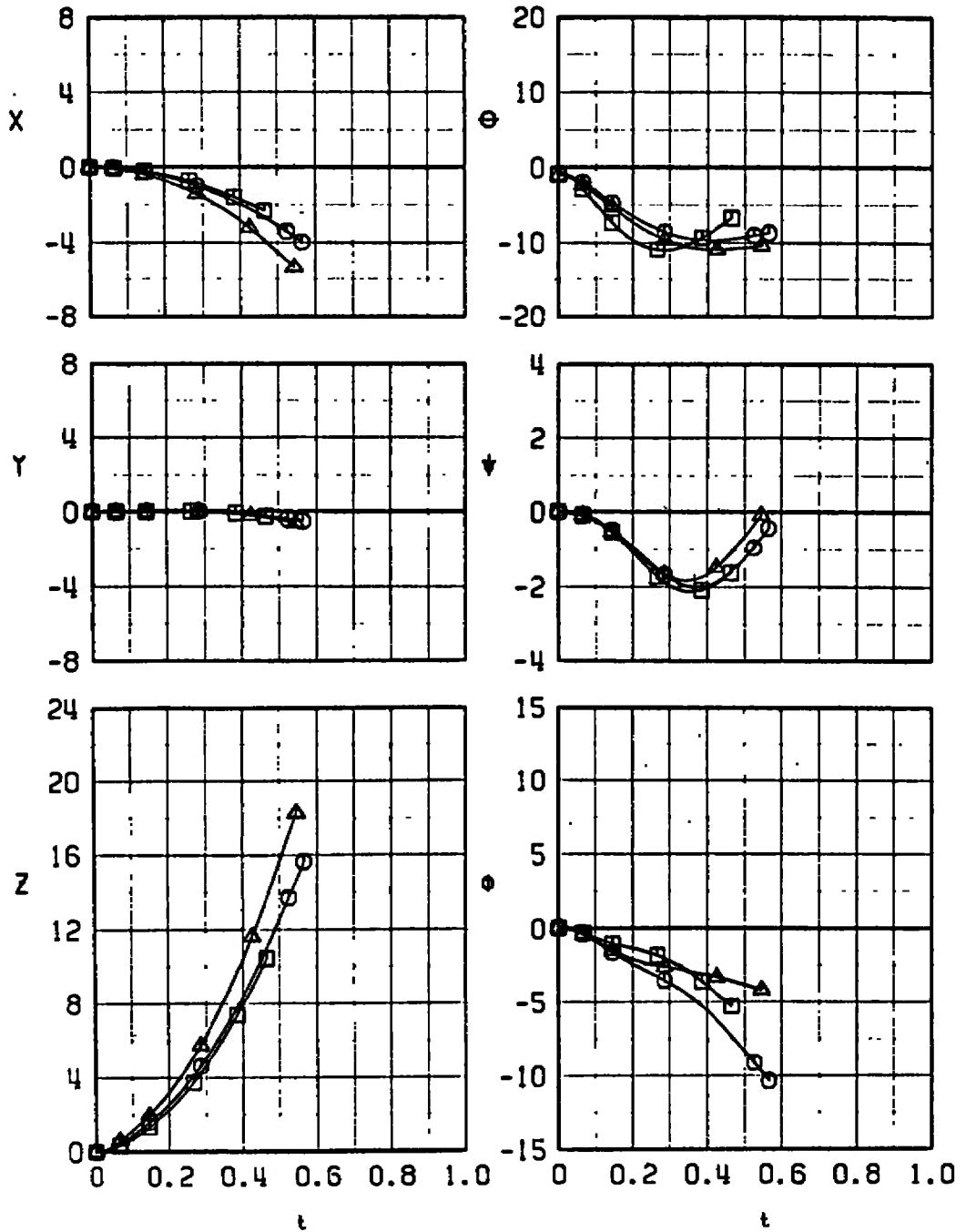


Fig. 13 Combined Mass and Center-of-Gravity Effects on Separation Trajectories for  $M_{\infty} = 0.87$  and  $\gamma = 0$  deg

SYM	CONF	$\alpha$	$\bar{m}$	$X_{cg}$
□	4	0.1	74.56	7.053
○	5	0.1	58.00	7.249
△	6	0.0	41.18	7.249



b. Pave Storm II  
Fig. 13 Concluded

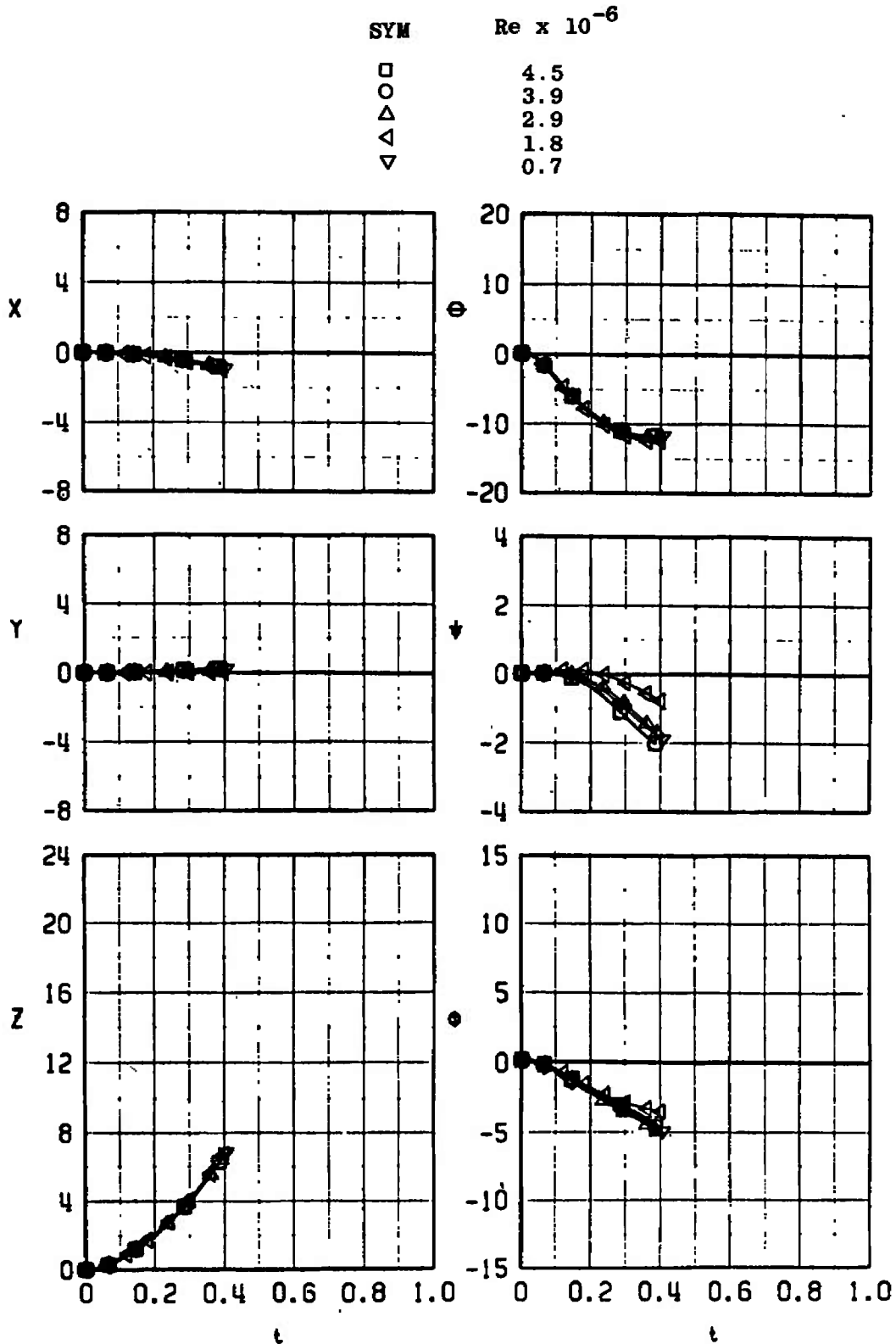


Fig. 14 Effects of Reynolds Number Variation in the Wind Tunnel on the Trajectories for Configuration 4,  $M_\infty = 0.70$ ,  $\alpha = 1.2$ , and  $\gamma = 0$

**TABLE I**  
**FULL-SCALE STORE PARAMETERS USED IN TRAJECTORY CALCULATIONS**

Configurations	Pave Storm I			Pave Storm II		
	1	2	3	4	5	6
Mass, $\bar{m}$ , slugs	70.373	48.300	36.680	74.565	58.000	41.180
Center-of-gravity location, $X_{cg}$ , ft	8.928	8.897	8.897	7.053	7.249	7.249
Center-of-gravity location, $Y_{cg}$ , ft	0	0	0	0.0042	0	0
Center-of-gravity location, $Z_{cg}$ , ft	-0.062	-0.090	-0.119	-0.058	-0.083	-0.107
Location of ejector force, $X_{L1}$ , ft	0.615	0.583	0.583	0.8875	1.083	1.083
Location of ejector force, $X_{L2}$ , ft	-1.053	-1.083	-1.083	-0.780	-0.583	-0.583
Ejector force curve (Fig. 9), $F_{Z1,2}$	a	c	b	a	d	b
Pitch moment of inertia, $I_{yy}$ , slug-ft <sup>2</sup>	438.0	351.3	317.6	397.5	423.0	364.4
Yaw moment of inertia, $I_{zz}$ , slug-ft <sup>2</sup>	435.8	357.3	317.6	495.6	423.0	364.4
Axial moment of inertia, $I_{xy}$ , slug-ft <sup>2</sup>	29.3	19.8	16.7	38.0	25.8	16.7
Product of inertia, $I_{xz}$ , slug-ft <sup>2</sup>	-0.26	-0.313	-0.395	-1.500	-2.056	-2.614
Pitch damping derivative, $C_{mq}$ , per radian	-275	-275	-275	-110	-110	-110
Yaw damping derivative, $C_{m\dot{r}}$ , per radian	-275	-275	-275	-110	-110	-110
Roll damping derivative, $C_{lp}$ , per radian	-20	-20	-20	-10	-10	-10

**TABLE II**  
**SUMMARY OF TEST CONDITIONS**

$\underline{M_\infty}$	$\underline{q_\infty}$	$\underline{\gamma, \text{deg}}$
0.50	500	0
0.54	500	0
0.70	790	0
↓	690	0
	500	0, 30, 60
	300	0
	125	0
	0.87	500
0.95	500	0, 30, 60

**TABLE III**  
**MAXIMUM FULL-SCALE POSITION UNCERTAINTIES RESULTING**  
**FROM BALANCE PRECISION LIMITATIONS AND ZERO SHIFTS**

$M_{\infty}$	t, sec	$\pm\Delta X$ , ft	$\pm\Delta Y$ , ft	$\pm\Delta Z$ , ft	$\pm\Delta\theta$ , deg	$\pm\Delta\psi$ , deg	$\pm\Delta\phi$ , deg
0.50	0.4	0.07	0.04	0.10	0.37	0.23	1.44
0.54	0.4	0.08	0.04	0.12	↓	↓	1.69
0.70	0.4	0.14	0.07	0.20			2.84
↓	0.6	0.55	0.16	0.46	↓	↓	6.40
0.87	0.4	0.21	0.11	0.32			4.41
↓	0.6	0.48	0.25	0.72			9.93
0.95	0.4	0.25	0.13	0.38	↓	↓	5.27
↓	0.6	0.57	0.30	0.85			11.85

**TABLE III**  
**MAXIMUM FULL-SCALE POSITION UNCERTAINTIES RESULTING**  
**FROM BALANCE PRECISION LIMITATIONS AND ZERO SHIFTS**

$M_{\infty}$	t, sec	$\pm\Delta X$ , ft	$\pm\Delta Y$ , ft	$\pm\Delta Z$ , ft	$\pm\Delta\theta$ , deg	$\pm\Delta\psi$ , deg	$\pm\Delta\phi$ , deg
0.50	0.4	0.07	0.04	0.10	0.37	0.23	1.44
0.54	0.4	0.08	0.04	0.12	↓	↓	1.69
0.70	0.4	0.14	0.07	0.20			2.84
↓	0.6	0.55	0.16	0.46			6.40
0.87	0.4	0.21	0.11	0.32			4.41
↓	0.6	0.48	0.25	0.72			9.93
0.95	0.4	0.25	0.13	0.38			5.27
↓	0.6	0.57	0.30	0.85	11.85		

## DOCUMENT CONTROL DATA - R &amp; D

(Security classification of title, body of abstract and indexing annotation must be entered when the overall report is classified)

1. ORIGINATING ACTIVITY (Corporate author) Arnold Engineering Development Center ARO, Inc., Operating Contractor Arnold Air Force Station, Tennessee		2a. REPORT SECURITY CLASSIFICATION UNCLASSIFIED	
		2b. GROUP N/A	
3. REPORT TITLE SEPARATION CHARACTERISTICS OF THE PAVE STORM I AND II FROM THE F-4C AIRCRAFT AT MACH NUMBERS FROM 0.50 TO 0.95			
4. DESCRIPTIVE NOTES (Type of report and inclusive dates) Final Report - June 7 to 11, 1971			
5. AUTHOR(S) (First name, middle initial, last name) A. C. Mansfield, ARO, Inc.		This document has been approved for public release its distribution is unlimited. Per TAB etc 16 August, 1971	
6. REPORT DATE September 1971	7a. TOTAL NO OF PAGES 59	7b. NO. OF REFS 2	
8a. CONTRACT OR GRANT NO. F40600-72-C-0003	9a. ORIGINATOR'S REPORT NUMBER(S) AEDC-TR-71-179 AFATL-TR-71-114		
b. PROJECT NO. 6033	9b. OTHER REPORT NO(S) (Any other numbers that may be assigned this report) ARO-PWT-TR-71-139		
c. Program Element 64212F			
d. Task 02			
10. DISTRIBUTION STATEMENT Distribution limited to U.S. Government agencies only; this report contains information on test and evaluation of military hard- ware; September 1971; other requests for this document must be referred to Armament Development and Test Center (DLGC), Eglin AFB, Florida 32542.			
11. SUPPLEMENTARY NOTES Available in DDC		12. SPONSORING MILITARY ACTIVITY ADTC (DLGC) Eglin AFB, Florida 32542	
13. ABSTRACT Wind-tunnel tests were conducted using 0.05-scale models to inves- tigate the separation characteristics of the Pave Storm I and II muni- tions from the F-4C aircraft. The separation trajectories were ini- tiated from the right-wing inboard pylon. Captive-trajectory store- separation data were obtained at Mach numbers from 0.50 to 0.95 for the parent aircraft in level flight, and 30- and 60-deg dive angles at a simulated altitude of 5000 ft. For the time period of the trajectories obtained, the store separated from the parent aircraft without store- to-parent contact.  Distribution limited to U.S. Government agencies only; this report contains information on test and evaluation of military hardware; September 1971; other requests for this document must be referred to Armament Development and Test Center (DLGC), Eglin AFB, Florida 32542.			

14.

KEY WORDS

LINK A

LINK B

LINK C

ROLE

WT

ROLE

WT

ROLE

WT

F-4C aircraft  
bombs (ordnance)  
Pave Storm  
separation characteristics  
trajectories  
transonic flow